



Comparison of SMILES ClO profiles with satellite, balloon-borne and ground-based measurements

H. Sagawa¹, T. O. Sato^{2,1}, P. Baron¹, E. Dupuy^{1,*}, N. Livesey³, J. Urban⁴, T. von Clarmann⁵, A. de Lange⁶, G. Wetzel⁵, B. J. Connor⁷, A. Kagawa¹, D. Murtagh⁴, and Y. Kasai^{1,2}

¹Applied Electromagnetic Research Institute, National Institute of Information and Communications Technology, Nukui-kita, Koganei, Tokyo 184-8795, Japan

²Tokyo Institute of Technology, Nagatsuta, Midori-ku, Yokohama, Kanagawa 226-8503, Japan

³Jet Propulsion Laboratory, California Institute of Technology, 4800 Oak Grove Drive, Pasadena, California 91109, USA

⁴Department of Earth and Space Sciences, Chalmers University of Technology, 41296 Gothenburg, Sweden

⁵Karlsruhe Institute of Technology, Institute for Meteorology and Climate Research, P.O. Box 3640, 76021 Karlsruhe, Germany

⁶SRON-Netherlands Institute for Space Research, Sorbonnelaan 2, 3584 CA, Utrecht, the Netherlands

⁷BC Consulting, 6 Fairway Dr., Alexandra 9320, New Zealand

*now at: National Institute for Environmental Studies, Onogawa, Tsukuba, Ibaraki 305-8506, Japan

Correspondence to: H. Sagawa (sagawa@nict.go.jp)

Received: 18 December 2012 – Published in Atmos. Meas. Tech. Discuss.: 17 January 2013

Revised: 18 October 2013 – Accepted: 5 November 2013 – Published: 6 December 2013

Abstract. We evaluate the quality of ClO profiles derived from the Superconducting Submillimeter-Wave Limb-Emission Sounder (SMILES) on the International Space Station (ISS). Version 2.1.5 of the level-2 product generated by the National Institute of Information and Communications Technology (NICT) is the subject of this study. Based on sensitivity studies, the systematic error was estimated as 5–10 pptv at the pressure range of 80–20 hPa, 35 pptv at the ClO peak altitude (~ 4 hPa), and 5–10 pptv at pressures ≤ 0.5 hPa for daytime mid-latitude conditions. For nighttime measurements, a systematic error of 8 pptv was estimated for the ClO peak altitude (~ 2 hPa). The SMILES NICT v2.1.5 ClO profiles agree with those derived from another level-2 processor developed by the Japan Aerospace Exploration Agency (JAXA) within the bias uncertainties, except for the nighttime measurements in the low and middle latitude regions where the SMILES NICT v2.1.5 profiles have a negative bias of ~ 30 pptv in the lower stratosphere. This bias is considered to be due to the use of a limited spectral bandwidth in the retrieval process of SMILES NICT v2.1.5, which makes it difficult to distinguish between the weak ClO signal and wing contributions of spectral features outside the bandwidth. In the middle and upper stratosphere outside the polar regions,

no significant systematic bias was found for the SMILES NICT ClO profile with respect to data sets from other instruments such as the Aura Microwave Limb Sounder (MLS), the Odin Sub-Millimetre Radiometer (SMR), the Envisat Michelson Interferometer for Passive Atmospheric Sounding (MIPAS), and the ground-based radiometer at Mauna Kea, which demonstrates the scientific usability of the SMILES ClO data including the diurnal variations. Inside the chlorine-activated polar vortex, the SMILES NICT v2.1.5 ClO profiles show larger volume mixing ratios by 0.4 ppbv (30%) at 50 hPa compared to those of the JAXA processed profiles. This discrepancy is also considered to be an effect of the limited spectral bandwidth in the retrieval processing. We also compared the SMILES NICT ClO profiles of chlorine-activated polar vortex conditions with those measured by the balloon-borne instruments: Terahertz and submillimeter Limb Sounder (TELIS) and the MIPAS-balloon instrument (MIPAS-B). In conclusion, the SMILES NICT v2.1.5 ClO data can be used at pressures $\leq \sim 30$ hPa for scientific analysis.

1 Introduction

Chlorine monoxide (ClO) is one of the key species for the ozone depletion mechanism in the stratosphere, participating in the reaction cycle as the primary element of the reactive chlorine family (e.g., Molina and Rowland, 1974). It has therefore been a major target of scientific interest for atmospheric observations. The global distribution of ClO has been observed by several satellite missions, for example, the Upper Atmosphere Research Satellite (UARS) Microwave Limb Sounder (MLS) (Reber et al., 1993; Waters et al., 1993) and its successor Aura MLS (Waters et al., 2006), the Odin Sub-Millimetre Radiometer (SMR) (Murtagh et al., 2002), and the Michelson Interferometer for Passive Atmospheric Sounding (MIPAS) (Fischer et al., 2008) onboard the Envisat satellite. There are also balloon-borne measurements such as the MIPAS-B2 gondola which supports the balloon-borne MIPAS instrument (Friedl-Vallon et al., 2004) and the Terahertz and submillimeter Limb Sounder (TELIS) (Birk et al., 2010) for the ClO measurements. From the ground, microwave radiometers such as the one operated at the Mauna Kea station, have been monitoring stratospheric ClO over 30 yr and providing important data sets not only for understanding atmospheric chemistry (e.g., Solomon et al., 1984) but also for validating other satellite measurements (e.g., Connor et al., 2007; Nedoluha et al., 2011; Connor et al., 2013).

The Superconducting Submillimeter-Wave Limb-Emission Sounder (SMILES) attached to the Japanese Experiment Module (JEM) on the International Space Station (ISS) performed ClO measurements with a sensitivity of an order of magnitude higher than other satellite-borne instruments due to its 4 K cooled superconducting receiver system (Kikuchi et al., 2010). Although its scientific findings are outside the scope of this paper, the SMILES ClO measurements provided several interesting insights into the stratospheric and mesospheric researches such as the global distribution of ClO in the middle atmosphere and its diurnal variations. In particular, these measurements observationally revealed the mesospheric diurnal variation of ClO for the first time (Sato et al., 2012).

The National Institute of Information and Communications Technology (NICT) in Japan has developed a retrieval processing chain for the SMILES data analysis. Sato et al. (2012) carried out a simulation study to assess the errors in the NICT-processed SMILES ClO profiles for the daytime mid-latitude condition. They concluded that systematic and random errors of 10–35 pptv and 30–40 pptv, respectively, are to be expected for each single retrieval of SMILES ClO at 30–50 km. For the mesosphere above 60 km (pressure ≤ 0.1 hPa), the error is dominated by the measurement error due to statistical measurement noise and the smoothing error introduced by the inversion analysis, resulting in the total error of 50–150 pptv. This error can be reduced to some extent by averaging several measurements at the expense of

the spatial and temporal resolutions. Averaging 100 profiles measured for the mesosphere can reduce the expected error to the systematic error limit (5 pptv at 0.1 hPa), which is attributed to bias uncertainties in the forward model parameters, specifically the spectroscopic parameters and instrument function.

In association with the error analysis by Sato et al. (2012), we intend in this paper to evaluate the quality of the SMILES ClO data generated by the NICT level-2 processing by comparing it with those obtained by the following instruments: Aura MLS, Odin SMR, Envisat MIPAS, TELIS, the balloon-borne MIPAS (MIPAS-B) and the ground-based radiometer at the Mauna Kea observatory. We also compare the NICT-generated data with the results from the SMILES operational level-2 processing developed by the Japan Aerospace Exploration Agency (JAXA). Comparisons with chemical model outputs are beyond the scope of this paper, but Khosravi et al. (2013) compared the ClO diurnal variations obtained by SMILES with their 1-D photochemical model and showed a general good agreement in terms of the relative amplitude of the diurnal cycle.

This paper is organized as follows. The SMILES instrumentation and retrieval procedure are described in Sect. 2. In Sect. 3, the results obtained using the NICT level-2 processor are compared with those derived from the JAXA level-2 processor. Comparisons with other instruments are made in Sect. 4. Finally, we summarize the key points in Sect. 5.

2 JEM/SMILES

2.1 Platform

SMILES was launched on 11 September 2009 and attached to the JEM on the ISS. Scientific measurements of trace gases using SMILES began on 12 October 2009 and continued until the malfunction of its submillimeter-wave local oscillator (21 April 2010). The ISS is in a non-sun-synchronous circular orbit with an inclination angle of 51.6° to the equator. The SMILES instrument was attached to the JEM with an orientation enabling its antenna field-of-view (FOV) to point in a 45° direction leftward from the ISS orbital motion. The latitudinal coverage of the SMILES observations was nominally between 65° N and 38° S. On days when the ISS was rotated by 180° around its yaw axis, SMILES observation latitude range shifted towards the Southern Hemisphere ($\sim 65^\circ$ S and 38° N). The ISS orbit period is ~ 91 min and the local time of the sub-ISS (nadir) point precesses with a full 24 h shift after a 1–2 months period. This enabled SMILES to observe the atmosphere under various local solar times.

Figure 1 shows the time evolution of the sampling density of ClO measured by SMILES under different solar zenith angle (SZA) conditions and for different latitudinal ranges. There were no ClO measurements during December 2009 due to the instrumental configuration. The measurement

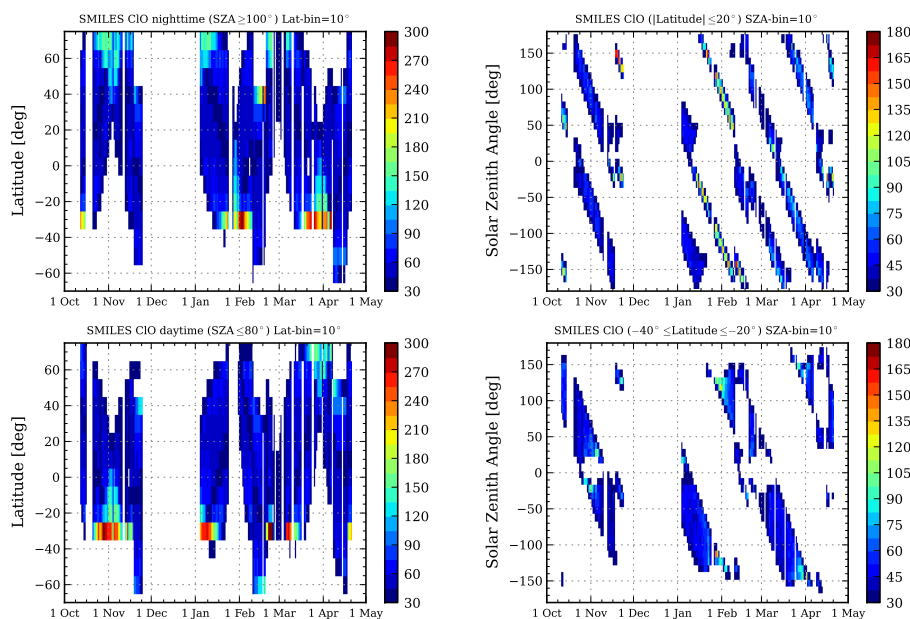


Fig. 1. Number of SMILES CIO measurements per day for the observation period (from 12 October 2009 to 21 April 2010). Left: measurement numbers summed over each latitudinal bin of 10° for each day. Upper and lower panels represent conditions for nighttime ($SA \geq 100^\circ$) and daytime ($SA \leq 80^\circ$), respectively. Right: measurement number as a function of observation date and SZA. Upper and lower panels show data for latitudinal regions of 20° S– 20° N and 40° S– 20° S, respectively. Note that the negative sign for SZA is simply an expedient representation used here which denotes the time range before noon.

density increases at both the northern and southern edges of the covered latitudes, where the ISS orbit shifts from ascending to descending. The plots in Fig. 1 illustrate that the sampling density and SZAs for each observation point varied significantly with the season and the latitude. An accumulation of SMILES data over several seasons without any special consideration would result in integrated data reflecting the inhomogeneous contributions from various SZA conditions. Such ISS-orbit induced characteristics should be kept in mind when observing short-lived species like CIO.

2.2 SMILES CIO observations

SMILES observes atmospheric emissions in limb-viewing mode via vertically scanning in a tangent height range from < 10 km to > 60 km. One vertical scan is conducted every 29.5 s, and one spectrum is obtained over 0.47 s data integration. The number of measurements (scans) is about 100 points per one cycle of the ISS orbit, which yields a nominal sampling density of about 1630 points per day. SMILES is operated in the specific frequency ranges: 624.32–625.52, 625.12–626.32, and 649.12–650.32 GHz (referred to Band-A, -B, and -C, respectively). The CIO transitions ($J = 35/2$ – $33/2$) at 649.445 and 649.451 GHz are observed in the Band-C configuration. The $40\text{ cm} \times 20\text{ cm}$ aperture of SMILES main reflector gives an instantaneous FOV of 0.089° (in elevation) in full width at half maximum (FWHM) corresponding to ~ 3 km at the tangent point. The main reflector

vertically scans the atmospheric limb at a rate of 0.009375° per 1/12 s, so the actual FOV for the 0.47 s-integrated measurement is a convolution of about six single FOVs. The submillimeter-wave signal is detected by the superconducting heterodyne receiver system which consists of two superconductor–insulator–superconductor (SIS) mixers associated with high electron mobility transistors (HEMT) amplifiers, and is then spectrally resolved by two acousto-optical spectrometers (AOS). The two AOSs detect Band-A, B, or C separately, enabling SMILES to observe two of the three bands simultaneously. Except for December 2009, when Band-C was not operated, the Band-C operation accounts for about 70 % of the total measurements (see Fig. 3 of Kikuchi et al., 2010). The frequency resolution of both AOSs is ~ 1.2 MHz at FWHM with a sampling step of ~ 0.8 MHz. The in-orbit system temperature of SMILES reached as low as ~ 350 K (Ochiai et al., 2010) and the effective noise root mean square (rms) level was ~ 0.5 K for one AOS channel (0.47 s integration).

The physical parameters (called level-2 products) are derived from the SMILES measurement spectra by solving the inverse problem. The operational level-2 product of SMILES measurement is processed by JAXA (e.g., Kikuchi et al., 2010; Suzuki et al., 2012). NICT developed another level-2 processing chain in order to investigate new alternatives for inversion algorithm (Baron et al., 2011). These products are called the “SMILES NICT level-2 products” and are the data products considered in this study. Version 2.1.5 of

the SMILES NICT level-2 product (hereafter denoted NICT v2.1.5 in this paper) was reduced from the calibrated spectra (level-1b product) of version 007. The NICT v2.1.5 processing chain employs a least-squares method involving a priori constraints (e.g., Rodgers, 1976, 1990, 2000). In this version, unlike the JAXA level-2 product, the NICT level-2 processing mostly targets the altitudes above ~ 25 km. Altitudes below have been less prioritized because of some level-1b calibration issues that have a strong impact in the lower altitudes. A vertical profile of the ClO volume mixing ratio (VMR) was derived for each scan using a spectral bandwidth of 400 MHz centered on the ClO line. Further details about the inversion methodology of NICT level-2 processor are found in the papers by Baron et al. (2011) and Sato et al. (2012).

Figure 2 shows examples of the ClO spectra from a single limb scan measured during the daytime (14:13 p.m. LT) at a low latitude (18.9° S) on 4 January 2010, and the VMR profile retrieved from that specific measurement. The original SMILES NICT v2.1.5 ClO product has an altitude-grid width of 3 km from 17.5 to 41.5 km, of 4 km from 45 to 53 km and of 5 km from 57.5 to 92.5 km. On the plot, the retrieved altitudes are converted to each corresponding pressure level. In the rest of this paper, we describe ClO profiles using pressure levels for the vertical coordinate in order to reduce the error on the altitudes (see Sect. 6.3 given by Baron et al., 2011). The conversion from altitude to pressure is performed for each SMILES measurement by using the a priori pressure profile. The a priori pressure profile is based on the data from the version 5.2 of the Goddard Earth Observing System Model (Rienecker et al., 2008) for 0–40 km and extrapolated upward to follow the hydrostatic equilibrium using the MSIS (Mass Spectrometer and Incoherent Scatter radar) temperature climatology data (Hedin, 1991). The quality of the retrieval can be assessed by considering the goodness of the fit as reported by the chi-squared statistics χ^2 after the retrieval, the averaging kernels, and the measurement response m . The definition of χ^2 in this paper is the summation of the squared and variance-weighted residual terms between the best-fitting spectra and the measurements as well as the deviation of the retrieved state from the a priori state, both normalized by numbers of measurements and retrieval parameters (see Eq. 2 given by Baron et al., 2011). Typical values of χ^2 for the SMILES NICT ClO profiles are around 0.5–0.8. Here, χ^2 being smaller than unity is because of the overestimation of the measurement noise (Baron et al., 2011). Averaging kernels describe the sensitivity of the retrieved ClO VMR to the true state of the atmosphere. Their vertical spread is used as an indication of the vertical resolution of the retrievals. The measurement response, which is the sum of the absolute values of elements of each averaging kernel, indicates the effect of the a priori state on the retrieved information (e.g., Baron et al., 2002; Merino et al., 2002). Hereafter, we use the following data selection thresholds to exclude extreme outliers: $\chi^2 \leq 0.8$ and $0.8 \leq m \leq 1.2$. By applying this data selection, approximately 12% of the total

measurements were discarded due to the χ^2 threshold. For a single-scan measurement, the SMILES NICT v2.1.5 ClO product has a satisfactory measurement sensitivity at a pressure range of ~ 80 –0.01 hPa (corresponding to altitudes of ~ 17 –80 km) with a typical vertical resolution of 3.5–13 km.

Figure 3 shows an example of ClO diurnal variation in the middle stratosphere (10 hPa) observed with SMILES. Two months of observations (January and February 2010) for the equatorial region were zonally averaged using a 1 h local time bin. Each vertical bar represents the $1\text{-}\sigma$ standard deviation of the measurements for each bin. For comparison, the ClO abundances obtained by Aura MLS, Odin SMR, and Envisat MIPAS for the same period are shown. Data from these other instruments are described in detail later (Sect. 4), as are the differences in the ClO VMRs. Here we note the small standard deviations (~ 6 pptv and 15 pptv for nighttime and daytime, respectively) for the SMILES ClO profiles that indicate the good sensitivity of SMILES observations. The lower panel of Fig. 3 shows the local-time evolution of the observed points over the two months. These results clearly show the benefit for SMILES of a non-sun-synchronous orbit: while the other instruments are onboard sun-synchronous satellites thus measuring only at fixed local times, SMILES samples a broad range of local time, allowing the instrument to effectively observe the diurnal variations of ClO.

2.3 Error analysis for the SMILES NICT ClO profiles

The systematic and random errors of the SMILES NICT v2.1.5 ClO product were investigated by Sato et al. (2012). They estimated the systematic error to be 35 pptv for the ClO peak altitudes (around 2–4 hPa) for typical daytime mid-latitude ClO profiles. This systematic error was dominated by the error due to an uncertainty in the pressure broadening parameter of the ClO spectral line. The previously reported known analytical problems for the presented version of the NICT ClO product are as follows: (1) the vertical movement of the SMILES FOV during a single spectrum integration of 0.47 s was ignored in the forward model; (2) an ideal rejection rate for the image sideband signal was assumed instead of using the actual characteristics of the sideband separation filter. Sato et al. (2012) showed that systematic errors of ~ 2 –4 and ~ 0.5 pptv were introduced at 2–4 hPa in the ClO profiles when ignoring the FOV vertical movement and the sideband filter characteristic, respectively, which are regarded as rather minor contributors to the total systematic error.

Here we performed an additional error analysis on the SMILES NICT ClO product for two specific measurement conditions: nighttime mid-latitude and chlorine-activated polar air. The reference ClO VMR profiles used in the simulation are shown in the left plot of Fig. 4. The error sources considered in this study are summarized in Table 1. These sources were selected as the most significant systematic error sources in the forward model according to the previous work by Sato et al. (2012). In addition to the error sources they

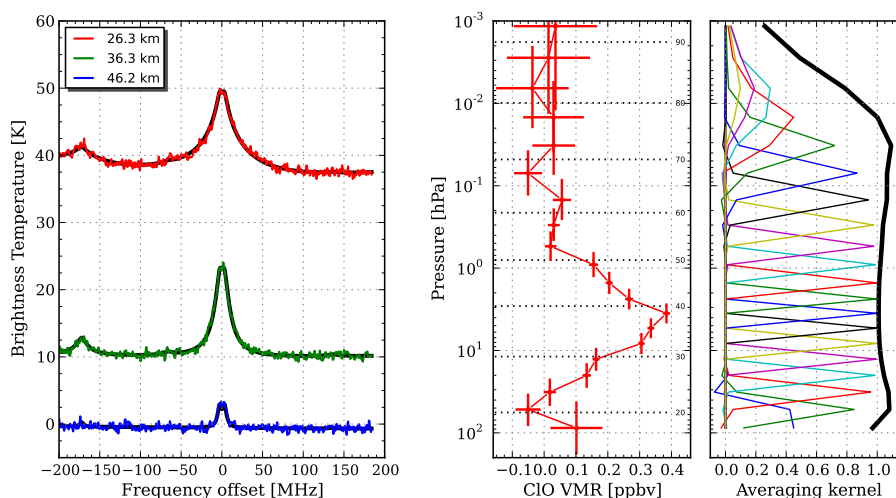


Fig. 2. Example SMILES CIO spectra, retrieved volume mixing ratio profile, and averaging kernels. Left: spectra from a single-scan observation obtained at (36° E, 18.9° S), local time of 14:13 p.m. on 4 January 2010. Spectra from only three-tangent heights are shown as examples. Background black lines represent best-fit synthesis spectra after inversion analysis. The frequency axis is shown as an offset from the mean frequency (649.448 GHz) of CIO doublet lines. The spectral feature observed at -180 MHz is an ozone isotope $^{17}\text{O}^{16}\text{O}$. Right: a sample CIO profile derived from a single-scan measurement, some of which are shown in the left panel, and the corresponding averaging kernels. Horizontal bars on CIO profile represent the $1\text{-}\sigma$ of the retrieval error, vertical bars indicate the vertical resolution of the retrieval which is estimated from the width of the averaging kernels. Small numbers along the right edge represent corresponding altitude levels in km. Rightmost plot shows averaging kernels and measurement response, i.e., envelope of each averaging kernel. Each thin colored line shows the averaging kernels for the retrieved state at different altitudes. The thick black line represents the measurement response of the retrieval.

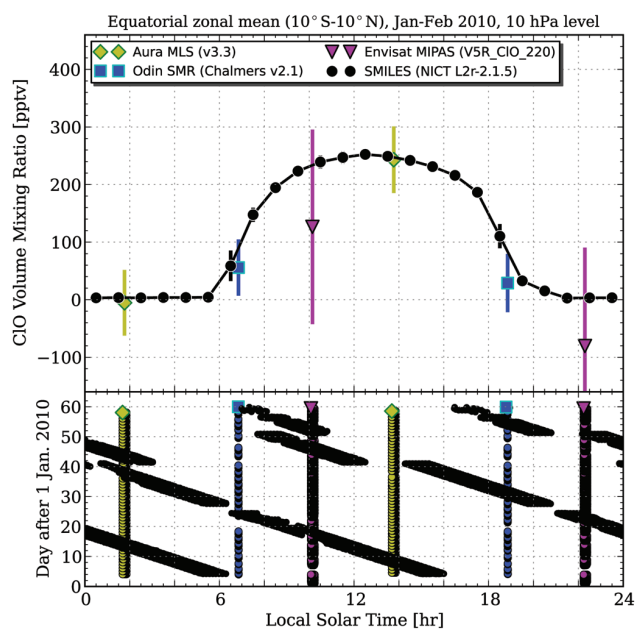


Fig. 3. Diurnal variation of CIO at 10 hPa observed by SMILES. Upper panel shows diurnal evolution of CIO VMR compared with measurements of Aura MLS, Odin SMR, and Envisat MIPAS. Vertical bars indicate the standard deviation ($1\text{-}\sigma$) of the retrieved VMRs. Lower panel shows the sampling density of measurements in the local time plane.

had investigated, we introduced a spectroscopic parameter error due to the uncertainty on transition frequency. This error was evaluated by testing retrievals with two values for the transition frequencies of the CIO doublet spectra: one from the JPL spectroscopic catalogue (Pickett et al., 1998; Cohen et al., 1984) (649.445040 and 649.451170 GHz), which was used in the original NICT v2.1.5 processing, and the other from the laboratory measurements of Oh and Cohen (1994) (649.445250 and 649.451072 GHz).

The null-space error also contributes to the systematic errors in certain conditions. NICT v2.1.5 processing uses fixed a priori values for CIO based on a typical daytime mid-latitude profile. This can introduce a systematic error for CIO retrievals under nighttime and chlorine-activated conditions where, in practice, CIO VMRs differ significantly from the assumed a priori daytime values. This impact was estimated in this study by calculating $(\mathbf{A} - \mathbf{I})(\mathbf{x}_{\text{ref}} - \mathbf{x}_{\text{a priori}})$, where \mathbf{A} is the averaging kernel matrix, \mathbf{I} the identity matrix, $\mathbf{x}_{\text{a priori}}$ the CIO a priori VMR used in the NICT v2.1.5 processing, and \mathbf{x}_{ref} the reference CIO profile assumed in the error analysis simulations. Since we added these error sources, we re-computed the error for the daytime mid-latitude conditions and checked the consistency with the previous results of Sato et al. (2012). Note that the null-space error was regarded as a random error for the daytime CIO retrievals, as discussed by Sato et al. (2012).

The right panel of Fig. 4 shows the estimated systematic errors for three typical CIO profiles. For each profile, the

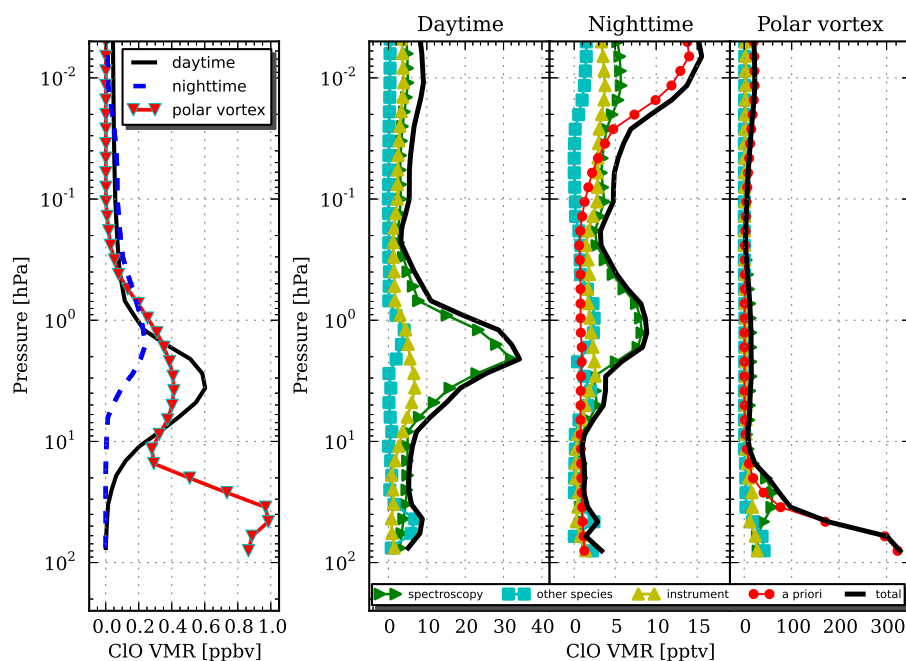


Fig. 4. Simulated systematic errors of SMILES ClO product (NICT v2.1.5). Left: reference ClO profiles used for synthesizing simulated spectra. Typical daytime, nighttime, and chlorine-enhanced polar air conditions were assumed. Right: estimated systematic errors for the considered ClO scenarios. See text for a description of the error sources.

Table 1. Systematic error sources considered in this study. See the text for detailed explanation about the inversion model error.

Error source	Assumed uncertainty
Spectroscopic parameters of ClO	
Transition frequency	footnote ^a
Line intensity	1 % (Pickett et al., 1998)
Air pressure broadening, γ	3 % (Cohen et al., 1984)
Temperature dependence of γ	10 % (Cohen et al., 1984)
Other absorption coefficient parameters in the radiative transfer model	
Dry air continuum	20 % ^b
Instrumental function	
Non-linearity correction of the gain	20% on the gain compression factor ^c
AOS response function	10 % of the FWHM (Mizobuchi et al., 2012)
Image sideband contamination	footnote ^d
Antenna scanning pattern	footnote ^e
Inversion model	
Null space error due to use of fixed a priori values	

^a Comparison between the transition frequencies from Cohen et al. (1984) and Oh and Cohen (1994). ^b Estimated by taking into account the roughness of the Pardo model (Pardo et al., 2001) which bases on a simple mathematical fit over a wide spectral domain (400–1000 GHz). ^c Private communication with S. Ochiai. See also Eq. (12) given by Sato et al. (2012). ^d Comparison between an ideal rejection rate for the image sideband signal and the realistic one. ^e Comparison between the cases with and without considering the vertical movement of the antenna FOV during a single spectrum integration.

considered systematic errors were divided into four components: error due to uncertainties in the spectroscopic parameters of ClO; error from other species in the radiative transfer model; error due to the uncertainty on the instrumental description in the forward model, including errors on the spectral gain calibration; and error from the use of a fixed a priori profile. The total systematic error was calculated as the root

sum square (rss) of individual error sources. From the simulation results, we obtained the systematic errors ($1-\sigma$ standard deviation of the bias uncertainty) shown in Table 2. In Table 2 we also included the $1-\sigma$ precision (random error) for a single-scan profile. For the daytime mid-latitude condition the systematic error was estimated as 5–10 pptv, 35 pptv, and 5–10 pptv for the lower stratosphere (pressure range of

Table 2. Summary of the systematic error and precision at selected pressure levels for SMILES NICT v2.1.5 ClO profiles. The relative systematic errors are shown in the parenthesis. Precisions are 1- σ standard deviation of the random error for a single-scan measurement. For the chlorine-activated polar vortex condition, only the errors for the lower stratosphere are shown.

Pressure	Daytime mid-latitude		Nighttime mid-latitude		Chlorine-activated polar region	
	Systematic [pptv]	Precision [pptv]	Systematic [pptv]	Precision [pptv]	Systematic [pptv]	Precision [pptv]
≤ 0.5 hPa	5–10 (6–20 %)	30–150	3–15 (5–30 %)	30–150	–	–
4–2 hPa	30–35 (10 %)	30–40	4–9 (5 %)	30–40	–	–
80–20 hPa	5–10 (≥ 10 %)	20–80	30 ^a (-%)	20–80	80–320 ^b (10–35 %)	30–160

^a Based on the actual negative VMRs in the retrieved profiles. ^b Errors for the pressure level of 30–80 hPa where the strong ClO enhancement occurs.

~ 80 –20 hPa), the ClO peak altitude (~ 4 hPa), and the upper stratosphere/lower mesosphere (pressure ≤ 0.5 hPa). These values are consistent with those presented by Sato et al. (2012), except for the lower mesosphere where the additional error due to the spectroscopic parameter is newly considered. For the nighttime mid-latitude condition systematic errors of 8 pptv and 3–15 pptv were estimated for the ClO nighttime peak altitude (~ 2 hPa) and the upper stratosphere/lower mesosphere (pressure ≤ 0.5 hPa), respectively. In the lower stratosphere (80–20 hPa), our estimated systematic error was less than 4 pptv. However, the actual SMILES NICT v2.1.5 ClO profiles have a more significant negative bias of about -30 pptv at 80 hPa (see details in Sect. 4.2.1). This implies that there are unimplemented or underestimated bias errors in the presented simulation, and for the scientific use of the SMILES NICT v2.1.5 data, we should take this observed negative bias into account. The systematic errors for the measurements of ClO activation in polar vortex were estimated to be 80–320 ppbv at a pressure range of ~ 30 –80 hPa assuming an enhanced ClO abundance of 1.0 ppbv, which mostly comes from the a priori contamination. This corresponds to a 10–35 % relative error.

3 Methodology of comparison

The SMILES NICT v2.1.5 ClO profiles were compared to (1) the SMILES ClO profiles processed by the JAXA level-2 chain (version 2.1), (2) the Aura MLS version 3.3 ClO profiles, (3) the Odin SMR ClO profiles from the version 2.1 of Chalmers level-2 processor, (4) the Envisat MIPAS IMK/IAA data version V5R_CIO_220, (5) the TELIS and MIPAS-B balloon-borne measurements, and (6) the ground-based microwave observations of ClO from the Mauna Kea station. Comparison-1 enables us to discern differences between the processing algorithms, since both the NICT and JAXA SMILES ClO profiles were processed from the same version (007) of the level-1b product. The target for 2–4 is a statistical comparison of the coincident geolocation measurements with those of satellite-based measurements for validating the SMILES ClO measurements at various local times in the lower and middle stratosphere. Comparison-5 with TELIS and MIPAS-B which flew within the northern

polar vortex, is aimed at evaluating the performance of SMILES ClO measurements under conditions of strong chlorine activation in the lower stratosphere. Comparison-6 with the ground-based measurements is tested to see if there is any impact from different observation geometry (i.e., limb viewing from the space and up-looking from the ground). Further information on each comparison data set is summarized in the following subsections, followed by the results of the comparison.

All comparisons were performed using the individual profile comparison approach, which has worked well for comparing various remote sensing observations (e.g., Dupuy et al., 2009). We searched all coincident measurement profiles (i.e., quasi-simultaneous observations in very close collocation) between the SMILES and comparison data sets. The basic criteria for the coincidence search between SMILES and other satellite instruments (MLS, SMR, and Envisat MIPAS) are set as follows: the distance of observation geolocation within 300 km, the difference in the observation time within 1 h, and the difference in the SZAs of the observed air mass less than 3° . The coincident measurements were searched for the day and night conditions separately by selecting the profiles with SZAs $\leq 80^\circ$ and $\geq 100^\circ$, respectively. The following modifications are applied to these basic criteria: for the Aura MLS case, thanks to the dense observation sampling of MLS, we could put a more stringent criterion for the geolocation distance as 100 km. For the comparison with Odin SMR, which measures the ClO during its fast and strong temporal variation near sunrise and sunset, we do not separate the a.m. and p.m. conditions; and for the comparison with Envisat MIPAS ClO, we discuss only the daytime profiles. The coincidence criteria for the balloon-borne instruments (TELIS and MIPAS-B) and the ground-based measurements will be described in detail at Sect. 5.4 and Sect. 5.5, respectively.

As discussed by Rodgers and Connor (2003), the differences in the averaging kernels and the a priori assumptions should be taken into account when comparing the results derived from different remote sensing instruments. We can see one of the most significant impacts of the different averaging kernels as the difference in vertical resolutions. Figure 5 shows the typical vertical resolution of ClO profiles

from different measurements used in this study. The vertical resolutions are defined based on the FWHM widths of each row of the averaging kernel matrices. It is shown that, in the middle stratosphere, the SMILES NICT v2.1.5 profiles have similar vertical resolutions with those of the SMILES JAXA level-2 product, MLS, and SMR: the vertical resolution of SMILES NICT v2.1.5 is 3.5–5 km at a pressure range of ~ 30 –1 hPa and 5–8 km at 1–0.1 hPa. It is 3–5 km at 200–0.1 hPa for the SMILES JAXA level-2 product; 3–4.5 km at 147–1 hPa for Aura MLS (Livesey et al., 2011); and 2.5–3 km at 100–1 hPa for Odin SMR (Urban et al., 2006). However, in the lower stratosphere (pressure ≥ 30 hPa) the vertical resolution of SMILES NICT v2.1.5 starts degrading to 5–8 km. In fact, the ClO profile measured by TELIS has a vertical resolution of 2–3 km in the lower stratosphere, which is more than twice better than that of the SMILES NICT v2.1.5 profiles, because it was situated within the atmosphere, which helps in significantly reducing the FOV of the measurement. On the other hand, the ground-based ClO measurements at Mauna Kea have a relatively broad vertical resolution of ~ 10 –17 km in the stratosphere. In order to take these differences in the measurement characteristics into account, we employed the following methods for the presented comparisons.

1. The comparisons with the JAXA level-2, MLS, and SMR on the outside of polar vortex were performed by directly using the original ClO profiles of each data set because of the similarity of their sensitivity to ClO. This is the same approach which was taken in the validation paper of Aura MLS ClO data (Santee et al., 2008).
2. For the comparisons of SMILES with the TELIS and ground-based ClO measurements (the cases where a clear difference in the vertical resolution can be seen), we convolved the averaging kernels of the lower resolution ClO profiles, \mathbf{A} , on the higher resolution profiles using the following function:

$$\mathbf{x}_{\text{smooth}} = \mathbf{A}\mathbf{x}_{\text{highres}} + (\mathbf{I} - \mathbf{A})\mathbf{x}_{\text{a priori}}. \quad (1)$$

$\mathbf{x}_{\text{highres}}$ represents the retrieved ClO profile from the higher vertical resolution instrument, and $\mathbf{x}_{\text{smooth}}$ is the same but after convolution with the lower resolution averaging kernels. $\mathbf{x}_{\text{a priori}}$ is the a priori profile used in the lower resolution processing. More specifically, for the comparison between SMILES and TELIS, we convolved the SMILES averaging kernel on the TELIS ClO profile in order to obtain the smoothed TELIS ClO profile; and for the SMILES and ground-based comparison, we convolved the ground-based measurement's averaging kernel on the SMILES profile to get the smoothed SMILES ClO profile. We also employed this convolution when ClO profiles from the polar vortex were targeted in the comparison, that is,

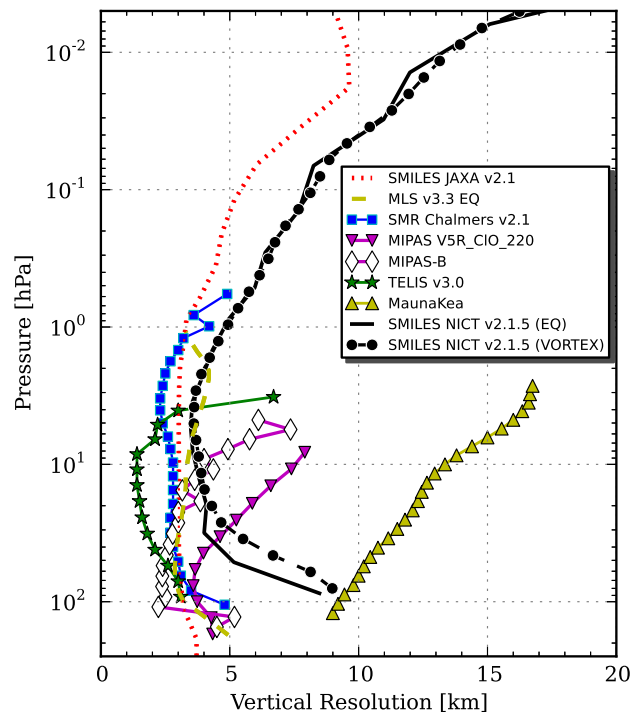


Fig. 5. Vertical resolutions of ClO measurements from the data sets considered in this study. Those for SMILES NICT v2.1.5 are shown in black lines for the equatorial region (solid line) and the chlorine-activated polar vortex condition (dotted-dashed line). The label “SMILES JAXA” represents the SMILES ClO product from the JAXA level-2 chain, taken from the equatorial region. The resolution of the JAXA level-2 ClO inside the polar vortex is almost equal to the equatorial one shown here. The vertical resolution of MIPAS-B is that for the retrieval using averaged measurements (see Sect. 5.4).

the comparison between SMILES NICT processing (lower resolution) and the JAXA processing (higher resolution) in Sect. 4.2.2.

3. The Envisat MIPAS and MIPAS-B profiles both have higher vertical resolutions than SMILES NICT v2.1.5 ClO in the lower stratosphere, however their ClO signals are weak in the observed infrared region causing relatively low amplitudes of the averaging kernels (peak values of the averaging kernels are smaller than 0.4 at pressure $\leq \sim 50$ hPa). In this study, we discussed the comparisons based on the smoothed ClO profiles: SMILES profiles were convolved with the averaging kernel and a priori assumptions of the Envisat MIPAS or MIPAS-B profiles, and the Envisat MIPAS and MIPAS-B profiles were convolved with the averaging kernel and a priori constraints of SMILES.

Once coincident profiles were found, then we applied the above-mentioned averaging kernels and a priori profile convolutions for individual profile (if necessary). The vertical

grid is linearly interpolated on a reference vertical grid which is arbitrarily determined. Absolute difference of the coincident pair was calculated as SMILES NICT—comparing data set. The median of the differences of each coincident pair was calculated to obtain a representative absolute difference profile for the considered comparison. To be less sensitive to outliers, we use the median statistic instead of the mean statistic to derive the average state. The variability of the compared data sets was estimated by calculating the median absolute deviation (hereafter abbreviated to MAD) values. The average relative difference was obtained by first calculating the individual relative differences on the basis of the ratio of the difference to the mean of the compared pair of CIO profiles. Then we took the median of those relative differences over the full set of coincident pairs.

The results of the comparisons are discussed taking the systematic errors of each instrument into account. The error budgets are based on the error analyses and validation studies of each instrument. The systematic errors on the difference between two instruments are estimated as the rss of the 1- σ error on each profile. For the comparisons of CIO profiles convolved with averaging kernels, the systematic errors are also convolved in the same way (i.e., the error covariance is calculated as $\mathbf{A}_1 \mathbf{S}_{x2} \mathbf{A}_1^T + \mathbf{A}_2 \mathbf{S}_{x1} \mathbf{A}_2^T$). Here \mathbf{A} and \mathbf{S}_x is the averaging kernel and systematic error covariance matrices, respectively, with the subscript 1 and 2 representing the different instrument.

4 Comparison of NICT v2.1.5 and JAXA level-2 profiles

4.1 Differences in the processing algorithms

The SMILES level-1b data are analyzed by two level-2 processors by JAXA and NICT, independently. These two level-2 processors have been developed as an independent research activity to investigate different retrieval strategies in order to exploit the full potentiality of the SMILES instrument. The retrieval algorithm is described by Baron et al. (2011) and by Suzuki et al. (2012) for NICT and JAXA level-2 processing, respectively. Here we performed a SMILES-internal comparison between the NICT v2.1.5 product and the JAXA level-2 product (version 2.1, 007-08-0310)¹ as a first-step check to evaluate the impact of differences in the two level-2 processing algorithms. Although both algorithms are based on the least-squares method using regularizations, there are six major differences in the forward model parameters and also in the retrieval configurations:

1. Spectral range of the measurements used in the inversion calculation: the JAXA level-2 processing uses the full bandwidth (1.2 GHz) of the Band-C spectrum, simultaneously retrieving CIO and other trace gases

¹Documentation is available at http://smiles.isas.jaxa.jp/access/SMILES_L2_product_v2-1_release_note.pdf.

such as HO₂, while the NICT v2.1.5 processing uses a limited bandwidth (400 MHz) centered on the CIO line. As discussed by Baron et al. (2011), using a narrower bandwidth degrades the sensitivity to lower altitudes since the information at those low altitudes, i.e., high pressure levels, is spread out in the far wings of the CIO emission line (see Appendix A for a discussion of the impact of the bandwidth on CIO sensitivity).

2. Correction of the AOS frequency offset: AOS frequencies are corrected with an offset parameter through the retrieval calculations in the NICT v2.1.5 processing, while they are fixed in the JAXA v2.1 processing.
3. Spectroscopic parameters used in the forward model, in particular, the line frequency ν_0 , the air broadening coefficient γ_{air} , and its temperature dependence n_{air} : the JAXA v2.1 processing uses coefficients based on Oh and Cohen (1994) ($\nu_0 = 649.445250$ and 649.451072 MHz, $\gamma_{\text{air}} = 2.11$ MHz mbar⁻¹, i.e., 2.81 MHz Torr⁻¹, and $n_{\text{air}} = 0.85$), while the NICT v2.1.5 processing uses the JPL catalog frequencies (Cohen et al., 1984) and the air broadening coefficients from laboratory experiments ($\nu_0 = 649.445040$ and 649.451170 MHz, $\gamma_{\text{air}} = 2.86$ MHz Torr⁻¹, and $n_{\text{air}} = 0.77$; see details in the paper by Baron et al., 2011).
4. CIO a priori profiles: the JAXA level-2 processing employs the monthly, latitudinal, day-night separated mean CIO profiles of the Aura MLS v2.2 product. The NICT v2.1.5 processing uses a single common profile for all observations. The a priori uncertainty is set as 100 % of the a priori value for the JAXA processing, while it is ~60 % for NICT.
5. Correlation length of the retrieval vertical layers (i.e., non-diagonal components of the a priori covariance matrix): 10 and 6 km are used in the JAXA v2.1 and NICT v2.1.5 processors, respectively.
6. Correction approach of the LOS elevation angles (i.e., tangent point heights): both processors retrieve an offset parameter for the LOS elevation angles within a single scan but in a different way. The JAXA level-2 processing uses the result of tangent point retrieval from Band-A or -B, which contains the strong O₃ transition at 625.371 GHz, as a priori value for retrieving the LOS elevation angle offset of the Band-C spectra. In contrast, the NICT v2.1.5 processing does not link the information from Band-A or -B to the retrieval of Band-C in order to avoid propagating any systematic errors between the two bands. It retrieves an LOS elevation angle offset from the CIO spectra, for which most of the information comes from the continuum baseline.

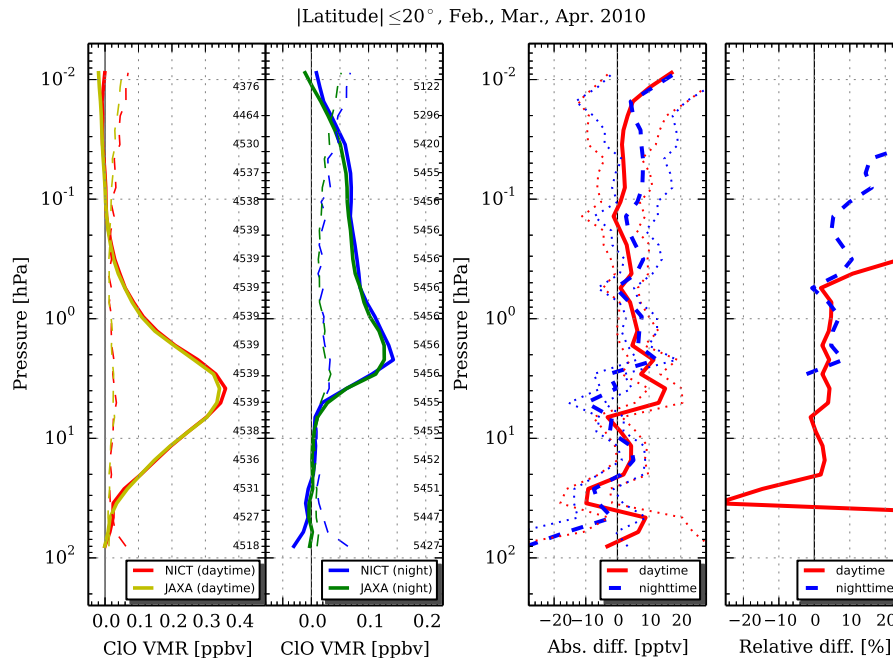


Fig. 6. Comparison of NICT v2.1.5 and JAXA v2.1 CIO profiles. Median VMR profiles are shown in the left panels. Daytime and nighttime data were separately averaged. Dashed lines show the 1-MAD of each data set. Small numbers along the right vertical axes represent numbers of coincidence at that altitude level. Right two panels show absolute (left side) and relative (right side) differences between the two data sets.

As shown in Fig. 5, the vertical resolution of the JAXA CIO product is slightly better than those of NICT v2.1.5.

4.2 Results

4.2.1 Comparison at the middle and low latitudes

Figure 6 shows the comparison between the CIO profiles from NICT v2.1.5 and the JAXA level-2 v2.1 products for equatorial latitudes (20°S – 20°N) in February–April 2010. We compared the day and night profiles separately by selecting the profiles with SZAs $\leq 80^{\circ}$ and $\geq 100^{\circ}$, respectively. There were 4539 and 5456 measurements for the day and night conditions, respectively. The left two panels show the median VMRs of the selected CIO profiles, for the day and night cases, with 1-MAD values (dashed lines). Medians of the absolute and relative differences are shown in the right panels. The dotted lines around the absolute difference profiles correspond to the 1-MAD of the individual absolute difference of each pair. The relative difference is plotted with a focus on the region around the peak in CIO concentration, i.e., at altitudes around 0.3–20 hPa and 0.03–3 hPa for the day and night profiles, respectively.

At the CIO peak altitudes (pressure levels of 4 and 2 hPa for day and night, respectively), the NICT v2.1.5 CIO profile shows larger VMRs than the JAXA-processed one; in detail, the differences are 15 and 10 pptv (or about 5 %) for day and night, respectively. Although these discrepancies between the daytime and nighttime profiles are within or comparable

to the estimated $1\text{-}\sigma$ bias uncertainty of the v2.1.5 product, we are interested in knowing whether such discrepancies can be explained by the use of different spectroscopic parameters in the two forward models. To investigate this, we randomly selected a sample of 200 SMILES level-1b scans from the equatorial daytime measurements for one day (4 January 2010), and processed them using the spectroscopic parameters of the NICT v2.1.5 forward model and using those of the JAXA level-2 processing. By replacing the spectroscopic parameters (transition frequency, γ_{air} , and n_{air}) with those used in the JAXA processing, the CIO VMR was decreased by ~ 7 pptv at 1–2 hPa but no significant change was observed at 4 hPa where we have seen the largest difference between the NICT v2.1.5 and the JAXA v2.1 CIO products. This suggests that the difference between the NICT and the JAXA CIO profiles is not solely due to the different spectroscopic parameters, but is rather a result of other factors that remain to be identified. Further investigation of this difference is currently under way, using a new version of the calibrated spectra. It should be mentioned that we saw a significant improvement in the residual of the best-fit spectra when the transition frequencies from Oh and Cohen (1994) were used. Such an error on the transition frequency is especially significant for observations of the mesosphere where the spectral line shape becomes narrower and weaker.

In the nighttime lower stratosphere (at pressures ~ 30 – 10 hPa) where CIO abundances are known to be nearly zero outside the polar region, the NICT v2.1.5 CIO profiles

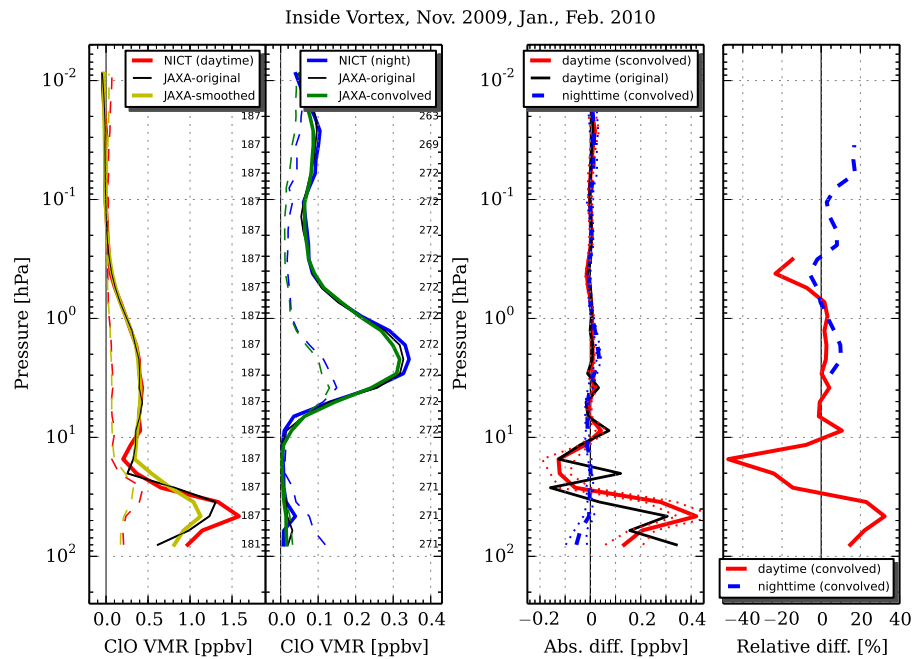


Fig. 7. Same as Fig. 6 except for polar vortex conditions. The thin black lines in the left panels represent the JAXA level-2 profiles with the original vertical resolution, and the bold lines are the same but after convolving the averaging kernel and a priori constraint of the NICT processing. The absolute difference for the daytime condition is shown in the original and smoothed vertical resolution comparisons, respectively.

show negative VMRs of about -30 pptv. As mentioned in Sect. 2.3, this negative bias is slightly larger than our estimated bias uncertainty. The increase of 1-MAD values, i.e., increase of variability of the NICT v2.1.5 ClO data at those altitudes, indicates that the retrieval processing has some problems. The reason for this negative bias is thought to be the limited spectral bandwidth used in the NICT processing. Using such a relatively narrow bandwidth introduces a contamination from other broadened spectral lines which cannot be distinguished from the ClO spectral signal. The NICT level-2 processing team is now working to solve this issue by implementing analyses based on the full bandwidth of SMILES spectra.

4.2.2 Comparison in the polar region

We also compared the ClO profiles obtained in polar vortex conditions observed in the Arctic winter of November 2009–February 2010 (December is omitted due to the non-operation of ClO measurement). The vortex-air measurements were selected by referring to the longitude and latitude information of the vortex obtained from the MLS-derived meteorological products (DMP) (Manney et al., 2007). We selected the SMILES data which measured within the “inner” vortex defined by MLS-DMPs (for the definition of the inner vortex edges, see the paper by Manney et al. (2007) and the references therein). As shown in Fig. 7, an enhancement of lower stratospheric ClO due to chlorine activation is clearly

seen in the SMILES profiles (both in daytime and nighttime conditions). When we smoothed the JAXA ClO profile to the vertical resolution of the NICT profile using the averaging kernel and the a priori profile of the NICT processing, the difference becomes more significant at the peak altitude of this lower stratospheric ClO enhancement. The difference was 0.4 ppbv (30 %) at 50 hPa for daytime conditions (measurements with SZAs $\leq 87^\circ$ were used in this daytime comparison at the polar vortex in order to increase the number of coincidences and also to select the data with strong ClO enhancements so that we can investigate the worst case of the systematic errors). This is significantly larger than our simulated systematic error (0.2 ppbv or 20 % as shown in Fig. 4). As we discussed in the previous sub-section, the NICT v2.1.5 processing is not optimized for retrieving ClO in the lower altitude because of a limited use of the spectral bandwidth. We consider that the shown positive bias for NICT v2.1.5 ClO is affected by this degradation of the sensitivity which introduces errors from spectral features outside the bandwidth and also a relatively larger contamination from the incorrect a priori ClO profile. Similar to the negative bias in the nighttime mid-latitude retrievals, this problem will be considered in the next version of the NICT level-2 processing. The characteristics of the ClO profiles under polar vortex conditions will be discussed further when we compare the SMILES measurements to those of TELIS and MIPAS-B (Sect. 5.4).

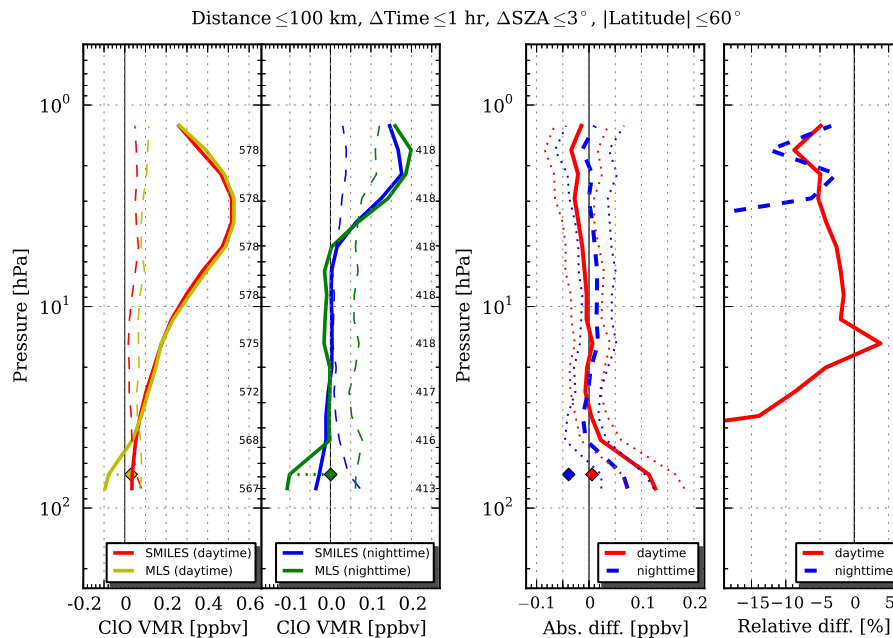


Fig. 8. Comparison of SMILES NICT CIO data with that of Aura MLS v3.3. Plot format is similar to that of Fig. 6. Diamond symbols on the CIO VMR profile plots represent MLS CIO VMRs after correcting for known bias for 68 hPa level (see text). The absolute differences between SMILES and the bias corrected MLS data at 68 hPa are also shown in diamond symbols.

5 Comparison with other instruments data sets

5.1 Comparison with Aura MLS v3.3 data

The Microwave Limb Sounder (MLS) onboard NASA's Earth Observing System (EOS) Aura satellite has been operating since 2004 (Waters et al., 2006). The satellite was launched into a near polar sun-synchronous orbit with the equator crossing local times of 13:45 (ascending) and 01:45 (descending). Aura MLS observes CIO with a radiometer centered at 640 GHz; that is, the same CIO transition that SMILES measures, though the frequency resolution is lower than that of SMILES. The frequency resolution is 6 MHz at the line center channels and increases to 96 MHz at the band edge. The system noise temperature is ~ 4200 K in double side-band receiver mode (Waters et al., 2006).

The CIO abundances were retrieved from the MLS measurement data using the optimal estimation method. The retrieval algorithm used was that reported by Livesey et al. (2006). The retrieved CIO profile is provided with a pressure grid ranging from 1000 to 10^{-5} hPa. A remarkable feature of their data processing is that not only the vertical profile information of the CIO, but also its horizontal distribution, is retrieved by combining consecutive limb scan measurements (the FOV of MLS is set in the forward direction of the Aura orbital motion, so consecutive measurements contain information from partially overlapping air masses). The observed data has been reprocessed using version 3.3 of the algorithm since 2011. In this version, the useful range for the

CIO profile is defined as 147 to 1 hPa (vertical resolution of ~ 3 –4.5 km) with a precision of ~ 0.1 –0.3 ppbv for a single scan (Livesey et al., 2011). The systematic error was estimated to be 0.025 ppbv at 15–1 hPa.

Santee et al. (2008) performed an intensive validation study for a previous version, version 2.2, of the Aura MLS CIO product. Their study showed that both the height of the peak in CIO profiles and its amplitude are well determined in the Aura MLS measurements, which makes the MLS data one of the best comparison partners for the SMILES data. For the lower stratosphere (typically pressures ≥ 22 hPa) significant negative VMRs were found for the MLS data set in both daytime and nighttime profiles. This negative bias problem was improved in the version 3.3 processing although altitude- and latitude-dependent biases of about -0.1 to $+0.6$ ppbv at pressure ≥ 68 hPa still need to be accounted for. The recommended correction values reported by the MLS team can be found in Livesey et al. (2011) and in the documentation on the MLS website².

Figure 8 shows comparison results between the SMILES and MLS CIO measurements. Coincidence measurements were searched for over the whole SMILES observation period in the low and middle latitude region (latitudes $\leq 60^\circ$). As described in Sect. 3, we defined three criteria for determining coincidence: observation points are closer than 100 km, observation time difference is smaller than 1 h, and

²http://mhs.jpl.nasa.gov/data/MLS_v3-3_CIO_BiasCorrection.txt.

the SZA difference is less than 3° . Using these criteria, we found 578 and 418 coincidences for daytime ($SZA \leq 80^\circ$) and nighttime ($SZA \geq 100^\circ$), respectively. The solid lines on the average VMR profiles for the MLS products are those before bias correction. There is a clear negative bias for the altitudes where pressure is larger than ~ 50 hPa. We applied the bias corrections suggested by the MLS team; the corrected VMRs are shown as symbols on the graph. After this correction, the daytime ClO profiles from both the SMILES and MLS showed a good agreement for the considered altitude range (100–1 hPa). The SMILES ClO VMR was smaller than the MLS one by ~ 0.04 ppbv (10 %) at the daytime peak altitude. This difference is within the combined (0.035 ppbv and 0.025 ppbv for SMILES and MLS, respectively) bias uncertainty.

For the nighttime case, the SMILES ClO data also showed negative VMRs for the lower stratosphere (~ -0.03 ppbv), as already pointed out by the SMILES-internal comparison. Except for this altitude region, the SMILES ClO measurements have nearly zero 1-MAD values, confirming that there is no ClO at these altitudes during the nighttime. This is a clear indication of the high sensitivity of SMILES measurement.

5.2 Comparison with Odin SMR v2.1 data

The Sub-Millimetre Radiometer, SMR, onboard the Odin satellite has been measuring stratospheric ClO since 2001 (Murtagh et al., 2002). Odin, an astronomical and aeronautical satellite mission by Sweden, France, Canada, and Finland has a circular sun-synchronous orbit (inclination angle of 97.8°), with equator-crossing local times of about 18:00 (ascending) and 06:00 (descending), respectively. The ClO transitions are observed at 501.3 GHz with a typical receiver noise temperature of 3000 K (single side-band).

The level-2 data processing of Odin SMR was divided into an operational processing at Chalmers University of Technology, in Sweden, and a research processing named CTSO (Chaine de Traitement Scientifique Odin) developed by a French team, though the CTSO processing chain is no longer operated now. The Chalmers ClO profile is retrieved at non-equidistant pressure levels corresponding to observation tangent points which interval is ~ 1.5 km and ~ 5 km at the altitudes below and above ~ 45 km, respectively (Urban et al., 2005). We used the recommended Chalmers operational ClO product, version 2.1, for comparison with the SMILES data. The bias uncertainty and the random errors were estimated to be smaller than 0.1 ppbv and 0.15 ppbv, respectively (Urban et al., 2006). These data were compared with the MLS ClO profiles (Santee et al., 2008; Livesey et al., 2011), which showed a good agreement in the middle stratosphere (pressure ≤ 46 hPa) having only a small difference of ~ 0.05 ppbv (SMR Chalmers-v2.1 VMRs are smaller than MLS) around 10 hPa. For the lower stratosphere, it was suggested that the SMR profiles may have a positive bias of 0.1 to 0.2 ppbv for the nighttime measurements outside the polar

vortex, when ClO abundances become smaller than the instrument sensitivity limit (Barret et al., 2006).

The number of the Odin SMR measurements are ≤ 975 per day, which is relatively smaller than those of SMILES and Aura MLS. To take this into account, we used the geolocation criterion of 300 km for coincidence determination. At low and middle latitudes, the Odin SMR ClO measurements are carried out near sunrise and sunset when the concentration of ClO drastically changes due to photochemistry. Therefore, the criterion for the SZA difference was kept as narrow as it was for the SMILES–MLS comparison. We identified 89 coincidences for the sunrise and sunset data in the low and middle latitudes (latitude $\leq 60^\circ$). Figure 9 shows the median ClO profiles and their differences derived from the coincident pairs of SMILES and SMR data. The difference between SMILES and SMR ClO profiles in the stratosphere is quantitatively consistent with that reported in the previous MLS–SMR comparisons (e.g., see Fig. 3.5.8 of Santee et al., 2008; Livesey et al., 2011). At the ClO peak altitudes (~ 2 hPa), the SMILES ClO VMR was larger than that of SMR by up to 0.05 ppbv, while in the lower stratosphere (pressure ≥ 30 hPa) the SMILES profiles had smaller VMRs by ~ 0.1 ppbv. What is new in our comparison result is the comparison in the lower mesosphere (pressure ≤ 1 hPa). Both SMILES and SMR observed the decrease of ClO VMRs with altitude above the 1 hPa level. At the 0.2 hPa level the SMR ClO profiles show unrealistic negative VMRs of -0.05 ppbv and therefore we cannot quantitatively conclude whether there is any systematic error in the SMILES data.

5.3 Comparison with Envisat MIPAS V5R_CIO_220 data

MIPAS onboard ESA's Environmental Satellite (Envisat) is a Fourier transform spectrometer operating in the spectral range of 4.15 to 14.6 μm (Fischer et al., 2008). It observed the atmospheric emission in the limb scanning geometry. The platform had a sun-synchronous orbit with an inclination angle of 98.55° . The equator crossing local times were around 10:00 (descending node) and 22:00 (ascending). The observations were performed from July 2002 to April 2012, with a discontinuity between April and December 2004 due to an instrumental anomaly. The observation mode (such as tangent height sampling of the limb and spectral resolution), which determines the data characteristics, was changed after this discontinuity. In this study we used version V5R_CIO_220 of the scientific level-2 product processed by the Institute for Meteorology and Climate Research (IMK) at Karlsruhe Institute of Technology, Germany.

The ClO data was retrieved from the weak 1–0 band at 11.8 μm using only P and Q branches, which are free of the overlapping contaminating HNO_3 emission. The profiles are retrieved on a vertical grid of 1 km grid width at altitudes up to 44 km, 2 km from 44 to 70 km, and 5 km from 70 to

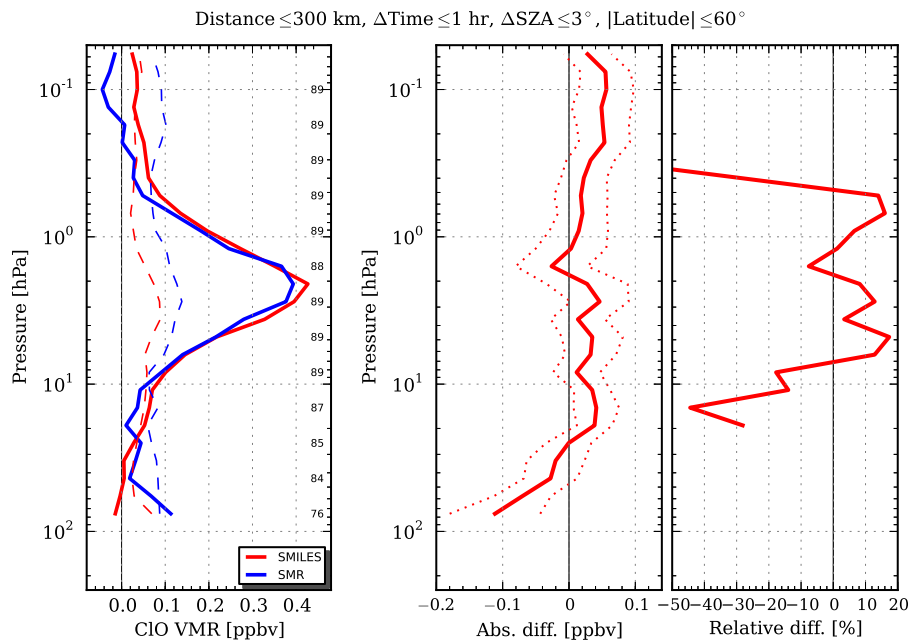


Fig. 9. Comparison of SMILES NICT CIO data with that of Odin SMR Chalmers-v2.1 product. Plot format is as similar as that of Fig. 6, except for not dividing the coincidences into daytime and nighttime cases.

120 km. Due to major overlap of the CIO lines with those of O_3 and CO_2 and the low sensitivity of MIPAS CIO measurements, this species had not been considered as a regular scientific data product in preflight sensitivity studies. Glatthor et al. (2004), however, showed that useful CIO distributions could be derived from MIPAS measurements under conditions of CIO enhancements. The scientifically usable altitude range reported in their paper was 10–30 km, but von Clarmann et al. (2005) have also detected CIO enhancements in the upper stratosphere. In 2004 a technical problem with MIPAS was encountered, and from 2005 until the loss of Envisat in April 2012, MIPAS measured at reduced spectral resolution. Total estimated retrieval errors are dominated by measurement noise, and range from 19 to 385 pptv in the altitude range from 10–30 km, which exceeds the 100 % limit between about 15 and 20 km (von Clarmann et al., 2009).

We selected the coincident measurements (geolocation distances within 300 km and the SZA differences within 3°) from latitudes lower than 60° , and focused only to the daytime conditions ($SZA \leq 80^\circ$) since the lower stratospheric CIO has very low abundances at the nighttime. In all, 780 coincidences were obtained, and they were compared after convolving the averaging kernels and a priori profiles of each of the other instruments as described in Sect. 3. The left two panels on Fig. 10 show the median CIO profiles from the SMILES NICT v2.1.5 and the Envisat MIPAS data in the original and convolved cases, respectively. The largeness of the 1-MAD of the Envisat MIPAS data comes from the limitation of the instrument sensitivity: it significantly increases

at pressure ≥ 30 hPa (altitudes below ~ 23 km) where the measurement error of Envisat MIPAS exceeds 100 %.

The absolute difference between SMILES and Envisat MIPAS is -50 to $+150$ pptv and -10 to $+60$ pptv for the original and convolved cases, respectively. In general, the Envisat MIPAS CIO is lower than the SMILES data (which is consistent to the result shown in Fig. 3). The combined systematic errors were estimated with taking the averaging kernel matrices of each instrument into account. The systematic errors of SMILES were taken from the daytime mid-latitude condition previously described in Sect. 2.3, and those of Envisat MIPAS were from the “ILS” and “spectroscopy” listed on Table 12 of the paper by von Clarmann et al. (2009). The estimated combined systematic error profile is shown as the black profile on the absolute difference panel of Fig. 10. It increases with altitude, being 30 pptv at 100 hPa and 70 pptv at 10 hPa. While the direct comparison of the original profiles (blue-dashed line in the absolute difference plot of Fig. 10) seems to hint at inconsistencies, after application of the averaging kernels as described in Sect. 3 the differences (solid red line) are almost fully explained by the estimated combined $1-\sigma$ systematic errors of both instruments (solid black lines).

The relative differences between SMILES and Envisat MIPAS were as large as -180 % (as shown at the rightmost panel of Fig. 10). The large percentage differences are, however, an artifact caused by the division of the absolute differences by the mean of the related SMILES and MIPAS profiles. Since MIPAS results are, due to the low sensitivity of MIPAS to CIO, biased low and show often negative

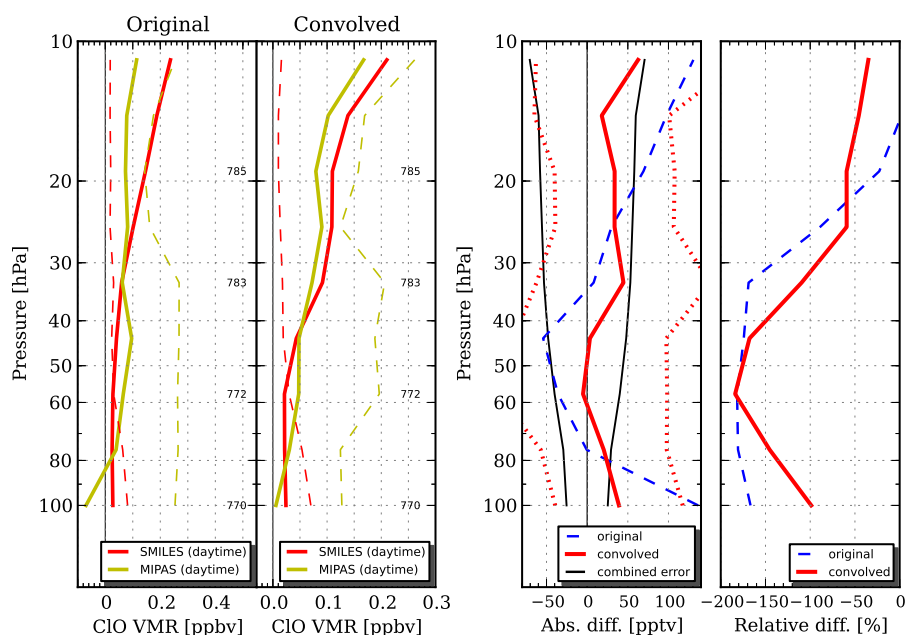


Fig. 10. Comparison of SMILES NICT CIO data with that of the Envisat MIPAS IMK V5R_CIO_220 product. Median daytime VMR profiles are shown in the left panels for the original level-2 products and those after convolving the averaging kernel and the a priori constraints of the each other instrument. Dashed lines show the 1-MAD of each data set. Small numbers along the right vertical axes represent numbers of coincidence at that altitude level. Right two panels show absolute (left side) and relative (right side) differences between the two data sets. The red dotted line on the absolute difference plot represents 1-MAD level, and the black line indicates 1- σ of the systematic errors after combining the errors from the both instruments.

values, this division causes unrealistically large percentage differences. The absolute differences contain much more reliable information.

5.4 Comparison with TELIS and MIPAS-B measurements inside the polar vortex

TELIS, the Terahertz and submillimeter Limb Sounder, is a balloon-borne instrument equipped with cryogenic heterodyne technology similar to SMILES. The balloon-borne Michelson Interferometer for Passive Atmospheric Sounding (MIPAS-B) is an advanced Fourier transform infrared spectrometer specially tailored to operate on a stratospheric balloon gondola. Both TELIS and MIPAS-B are mounted on the MIPAS-B2 gondola sharing the platform with the mini-DOAS instrument. In this configuration the gondola was launched in three consecutive winters (2009–2011) from Kiruna, Sweden. In this study only the second flight in 2010, when SMILES was operational, is considered. The balloon was launched on 24 January 2010 and remained aloft for about 13 h at a height of 34 km in Arctic polar vortex air (de Lange et al., 2012; Wetzel et al., 2012). TELIS vertically scanned the atmosphere with tangent heights ranging from ~ 9 km to 32.5 km with ~ 1.5 km step. A single scan takes about 50 s to complete.

TELIS was equipped with receivers operating at 480–650 GHz (de Lange et al., 2010) and at 1.8 THz. The CIO

profile was determined from the transition at 501.27 GHz, the same as SMR. The level-2 processing of the TELIS CIO measurements was done using the Tikhonov regularization (Tikhonov, 1963) described in detail by de Lange et al. (2012). Null values were used for an a priori of CIO profile, which is required to perform the averaging kernel convolution in this study. The retrieved profile has a vertical grid with 1.5 km interval. In that paper, the TELIS CIO and HCl products were compared with the coincident measurements of Aura MLS. The difference between the TELIS and MLS CIO (version 2.2) profiles in daytime equilibrium was ~ 0.2 ppbv at the CIO peak altitude, and was within the expected systematic errors of both instruments (de Lange et al., 2012).

With respect to MIPAS-B, its low-level data processing including instrument characterization is described by Friedl-Vallon et al. (2004). Retrieval calculations of MIPAS-B measurements were performed with a least squares fitting algorithm using analytical derivative spectra. The Tikhonov–Phillips regularization approach constraining with respect to the form of a height-constant zero a priori profile was adopted. The CIO retrieval was carried out in the P-branch region of the 11.8 μm band. The retrieved profile is output in a 1 km interval vertical grid with an altitude resolution of about 2–5 km. A further overview of the MIPAS-B data analysis is given by Wetzel et al. (2012) and references therein.

In this section we compare the SMILES NICT v2.1.5 ClO profiles with those from TELIS (version 3.0 of its level-2 product) and MIPAS-B. The TELIS profile used in this study includes a correction for the non-linear response function of the detector, which was absent in the previous TELIS–MLS comparison by de Lange et al. (2012). Figure 11 shows the close coincident measurement locations of SMILES, TELIS and MIPAS-B. The SMILES tangent points for a tangent height of 23 km are shown by the black square symbols, and those of TELIS by blue circles. The observation line-of-sight directions are also shown. It is noted that the longitude and latitude of the tangent points of SMILES single scan have almost negligible variability when compared to that of TELIS and MIPAS-B measurements. The SMILES measurement of the observation identifier 761 (tangent point at 30.5° E, 64.8° N) shows good coincidence with TELIS observations 14932 (32.4° E, 67.3° N), 17611 (33.6° E, 66.7° N), and 21537 (34.0° E, 64.7° N); the latter being the closest in terms of geophysical distance (~ 160 km). In case of MIPAS-B measurements, the sequences from 08a to 09b are the best candidates for comparison as these are conducted under virtually identical observation geometries as the TELIS observations 14932 and 17611. We used the MIPAS-B ClO profile that was retrieved from the averaged spectra of measurement sequences 08a–09b, improving the signal-to-noise ratios in the measurement which led to a higher vertical resolution. In addition, the SMILES measurement 760 (23.2° E, 64.0° N) shows good coincidence with the Aura MLS measurements shown by stars on the map, and therefore we also included them in this comparison. On the background of Fig. 11, the spatial distribution of the potential vorticity (PV) at the isentropic surface (potential temperature of 530 K which corresponds to approximately 28 hPa) is also shown in order to see the vortex activity at that day. The PV data were taken from the European Centre for Medium-Range Weather Forecasts (ECMWF) analysis for 12:00 UTC of 24 January 2010.

Figure 12 shows the ClO profiles derived from the SMILES, TELIS, MIPAS-B, and MLS measurements. As described in Sect. 3, we convolved the TELIS and MLS profiles with the SMILES averaging kernels (middle plot of Fig. 12), and for the comparison, including MIPAS-B, both of the SMILES and MIPAS-B averaging kernel matrices were considered (right plot of Fig. 12). In general the SMILES NICT v2.1.5 ClO profiles detected the ClO enhancement in the lower stratosphere to a satisfactory extent despite its limited sensitivity at these altitudes. The SMILES ClO VMR profiles from the measurements 760 and 761 are almost identical and show the largest ClO enhancement compared to the others. From the SMILES-averaging kernel convolved comparison it follows that the SMILES peak values are +0.4 ppbv (16 %) and +0.2 ppbv (8 %) respectively larger than TELIS and MLS (see the closeup at the sub-plot). The expected systematic error is ~ 10 % for both SMILES and TELIS at 25 hPa (~ 23 km) (de Lange et al., 2012). This corresponds to 0.25 ppbv (SMILES) and 0.2 ppbv (TELIS). After

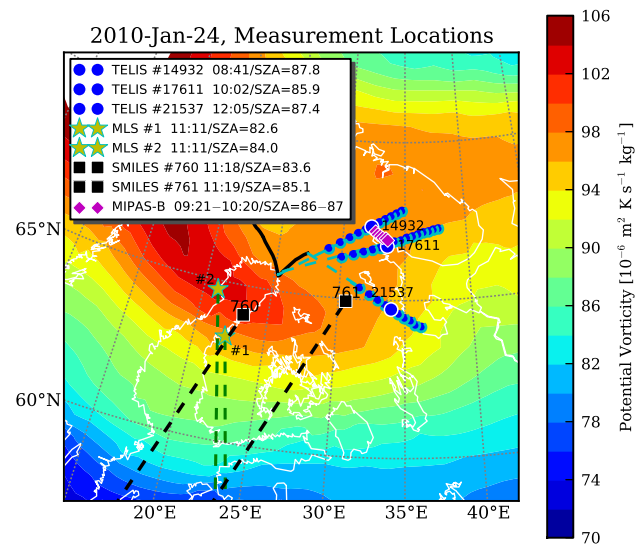


Fig. 11. Locations of selected SMILES, TELIS, MIPAS-B, and MLS measurements on 24 January 2010, superimposed on the potential vorticity distribution. Black squares represent SMILES measurement locations referring to the tangent point when SMILES pointed to a tangent height of 23 km. Observational lines-of-sight (LOS) are shown for the SMILES measurements as black dashed lines. The small number above each symbol is SMILES observation identification number. Corresponding local times and SZAs are indicated in the legend. Blue circles represent the tangent points of TELIS measurements, for which the vertical scan started at ~ 9 km. The black solid line represents the trajectory of the TELIS balloon gondola, and the blue dashed lines are the direction of the LOS towards each tangent point. The larger blue circles indicate the tangent points when TELIS looked at a tangent height of 23 km. Five-digit numbers on TELIS measurement locations indicate the observation identifier, with local time and SZA shown in legend. Stars represent two Aura MLS measurement locations with green dashed lines showing their LOSs. The measurement numbers for MLS are arbitrary ones prepared only for this study. MIPAS-B tangent points at 23 km for the measured sequences 08a–09b are shown as diamond symbols. The observation times and solar zenith angles changed from 09:21 to 10:20 and from 87° to 86° within those sequences (details can be found in the Figs. 1 and 2 given by Wetzel et al., 2012). The observation LOS is the same as that of TELIS 17611 measurement. The background color contour represents the potential vorticity (PV) field at the isentropic surface of 530 K (approximately 19 km), taken from the ECMWF analysis at 12:00 UTC on the same day as the observations.

convolving the TELIS systematic error with the SMILES averaging kernel, the combined systematic error of SMILES and TELIS was estimated 0.35 ppbv. The observed difference between SMILES and TELIS is larger than this combined systematic error. Below the ClO peak altitude the SMILES profiles become more similar to the MLS results, while at altitudes above the peak they show good agreement with those of TELIS. Looking to the comparison with MIPAS-B, the amplitude of ClO enhancement derived by

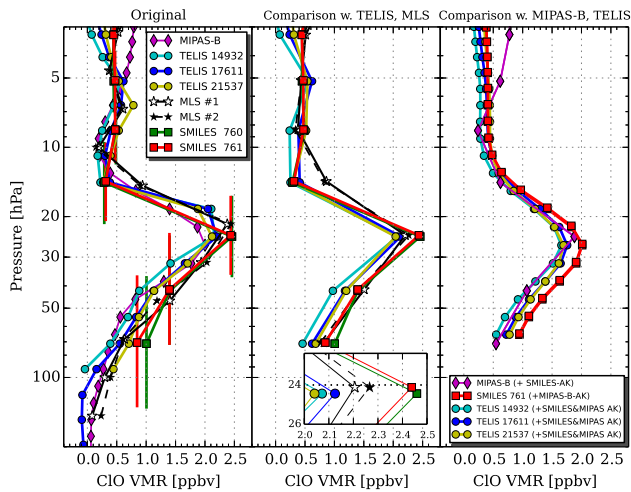


Fig. 12. CIO profiles derived from the SMILES v2.1.5, TELIS v3.0, MIPAS-B, and MLS v3-3 data. Left: original level-2 profiles without any smoothing. The vertical bars on the SMILES data indicate the vertical resolutions. Middle: TELIS and MLS profiles are convolved with the SMILES averaging kernels. Small sub-plot at the bottom of the panel shows the closeup at the CIO enhanced altitude. Right: comparison with the MIPAS-B CIO profile. The SMILES profile from measurement 761 is convolved with the MIPAS-B averaging kernel matrix, and the MIPAS profile is convolved with the SMILES averaging kernels. For the TELIS measurements both of the SMILES and MIPAS-B averaging kernel matrices are considered.

TELIS is fairly consistent with that derived by the MIPAS-B measurements. It is most likely that the SMILES NICT profiles have a positive bias in the lower stratosphere, which is consistent with the comparison with the SMILES JAXA level-2 product (see Sect. 4.2.2). It should be noted that the SMILES (and MLS) measurements are rather on the edge of the vortex (as shown by the strong gradient of the PV surface) with a horizontal resolutions of ~ 500 – 1000 km, and therefore even a small mismatch in the geolocations, SZAs, or in the observation LOS directions between the coincident profiles could yield variabilities of the CIO distribution along each instrument's LOS. Therefore, we consider it difficult to quantitatively discuss bias errors of SMILES CIO only from this coincidence comparisons. This situation can be improved by future studies using outputs of chemical models for statistical comparison.

5.5 Comparison with ground-based measurements at Mauna Kea

A ground-based microwave instrument located on Mauna Kea, Hawaii, has been monitoring stratospheric CIO almost continuously since 1992, as one instrument of the Network for the Detection of Atmospheric Composition Change (NDACC) (e.g., Solomon et al., 2006; Nedoluha et al., 2011; Connor et al., 2013). The millimeter heterodyne receiver

detects the CIO emission line at 278.632 GHz with a total bandwidth of 506 MHz. Data analysis algorithm has been recently revised by Connor et al. (2013). Atmospheric spectra are taken continuously over several consecutive days (\sim a week), where the daytime and nighttime spectra are collected from the observations at 09:00–17:00 and 22:00–05:00 local time, respectively. An averaged nighttime spectrum is subtracted from the averaged daytime spectrum in order to remove the interfering spectral lines and the spectral baseline curvature coming from instrumental artifacts. Such “daytime–nighttime” CIO spectra are inverted to deduce the CIO profile by an optimal estimation method with a single a priori profile. The output vertical grid has a constant interval of 3 km with a vertical resolution of 9–16 km. The usable altitude range is around 20–45 km (e.g., Solomon et al., 2006; Nedoluha et al., 2011). The random and bias error are estimated by Solomon et al. (2006) and the combined total error is 40, 35, 22, 36 and 37 pptv, for the altitude ranges of 20–24, 25–29, 30–34, 35–39, and 40–44 km, respectively.

Nedoluha et al. (2011) compared the Mauna Kea CIO measurements with the UARS and Aura MLS instruments for the data taken in 1991–2009. The difference between the ground-based and MLS measurements was about 7–8 % at the peak of the “daytime–nighttime” CIO, ~ 4 hPa (~ 40 km), which was within the $1\text{-}\sigma$ level of estimated systematic errors over most of the altitudes. The comparison with the MLS CIO data was also discussed in the paper by Connor et al. (2013). They used a re-analyzed version of the Mauna Kea ground-based data for the comparison, and obtained a good agreement within 35 pptv for 50–1 hPa range.

The CIO comparison between the SMILES NICT v2.1.5 and the Mauna Kea ground-based measurements was performed on the basis of “daytime–nighttime” CIO profiles. We searched the SMILES data within 500 km (300 km was not large enough to find coincident SMILES data) from the Mauna Kea observatory for the periods which the ground-based measurements had been carried out. The SMILES CIO data were separated into the daytime ($SZA \leq 50^\circ$) and nighttime ($SZA \geq 150^\circ$) conditions, and then the mean daytime and nighttime SMILES CIO profiles were calculated. The SZA requirement for the daytime data was set to be smaller than 50° in order to obtain the SMILES measurements when the diurnal variation of CIO becomes relatively constant (i.e., around noon). The nighttime criterion was set to be similar with the one used for the ground-based data analysis. This was important to reduce the comparison error associated with the diurnal variation of upper stratospheric CIO in nighttime. We found the coincident pairs of SMILES and the Mauna Kea ground-based data for the following 5 periods: 5–15 January, 3–12 February, 11–22 March, 3–7 and 8–17 April in 2010. By taking the difference of these daytime and nighttime CIO profiles, we obtained the “daytime–nighttime” CIO profiles for the SMILES measurements. These SMILES “daytime–nighttime” CIO profiles were smoothed to the ground-based resolution using the averaging kernel and the

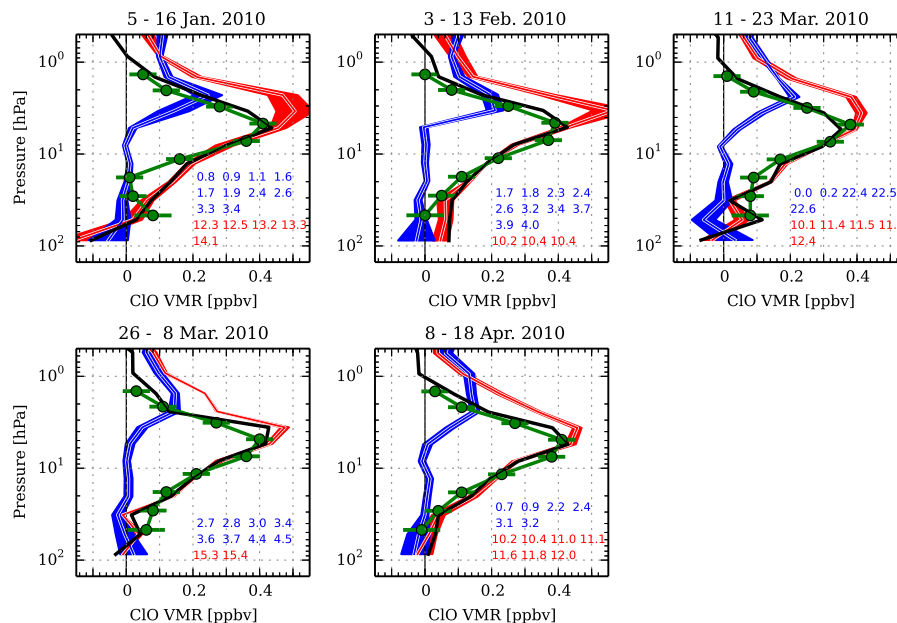


Fig. 13. Coincident SMILES NICT v2.1.5 ClO profiles and Mauna Kea measurements for the selected five period between 5 January and 18 April 2010. The red and blue profiles represent the mean daytime and nighttime SMILES ClO profiles, respectively, showing the $1\text{-}\sigma$ standard deviation of the selected profiles. The local times (h) for the SMILES data that are used for the averaging are shown at the lower right of each panel (blue and red fonts mean nighttime and daytime, respectively). Bold black profile is the mean “daytime–nighttime” SMILES ClO profile, and the green circles indicate the ground-based measurements. The error bars of the ground-based ClO profile represent the $1\text{-}\sigma$ retrieval errors.

a priori ClO profile of the ground-based measurements, as described in Sect. 3.

Figure 13 shows the SMILES NICT v2.1.5 ClO profiles (before smoothing) and the ground-based ClO profiles for the coincident periods. The period of the ground-based measurements is labeled as the title of each plot. The mean daytime, nighttime, and “daytime–nighttime” SMILES NICT, and the ground-based “daytime–nighttime” profiles are shown. Both SMILES and the ground-based profiles show the peak at the pressure level around 5–8 hPa which is at a slightly lower altitude than the daytime peak altitude. This is because the nighttime ClO is not zero at those altitudes. The comparison results for the smoothed SMILES profiles are shown in Fig. 14. In the lower right panel, the absolute differences between the SMILES and the ground-based “daytime–nighttime” ClO profiles are shown. In general, the agreement is very good. For most of the case, the absolute difference is within 35 pptv, which is similar as the agreement obtained by the ground-based and MLS comparison (Connor et al., 2013). The comparison for the period of 5–15 January shows the largest discrepancy (90 pptv at 20 hPa). Except this period, the differences are within the $1\text{-}\sigma$ of the systematic error over whole the considered altitude range.

6 Conclusion

SMILES has provided a unique data set of global (38°S – 65°N in the nominal case, and 65°S – 38°N during the specific yaw-maneuvered periods) ClO observations from the lower stratosphere up to the mesosphere. Its high sensitivity has revealed the distribution of ClO in the mesosphere and the non-sun-synchronous orbit allowed us to follow its diurnal variation. It is thus an important database for advancing our understanding of atmospheric chemistry.

We compared the SMILES ClO profiles processed at NICT with those generated by the JAXA level-2 chain, and with measurements of several satellite, balloon-borne, and ground-based instruments. The difference between the retrieval configurations of the NICT v2.1.5 and the JAXA operational code v2.1 processors resulted in a ClO difference of 15 pptv at 4 hPa for daytime and 10 pptv at 2 hPa for nighttime measurements. These differences are within the estimated systematic error of the NICT v2.1.5 processing. In the nighttime lower stratosphere where ClO VMRs are known to decrease to zero, the NICT v2.1.5 ClO profiles show negative VMRs of about -30 pptv. The cause for this bias is considered to be the use of the limited spectral bandwidth in the NICT processing which introduces contaminations from other broadened spectral signals. This seems to have also affected the NICT v2.1.5 ClO profiles from chlorine-activated polar vortex conditions, where the NICT v2.1.5

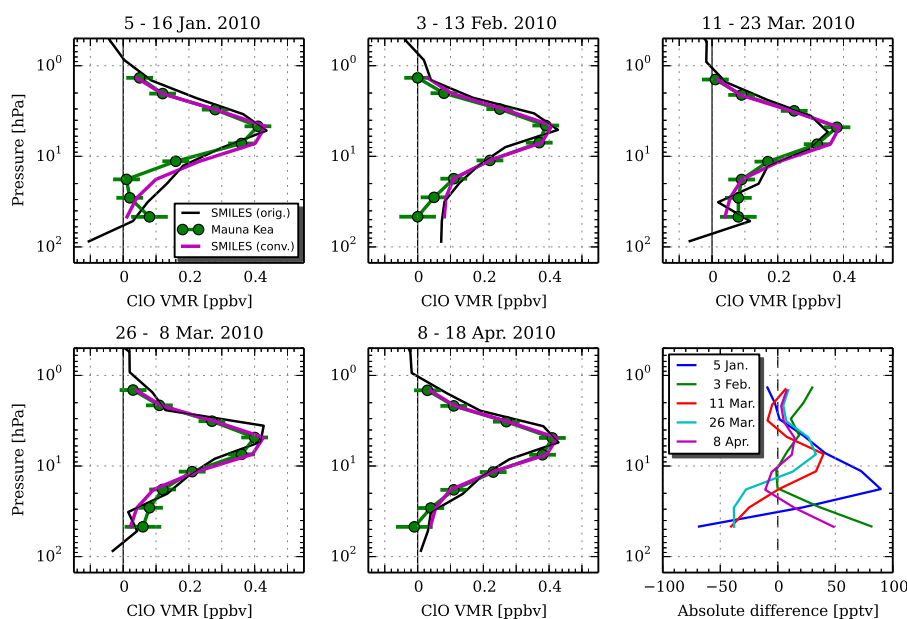


Fig. 14. Comparison between the SMILES NICT v2.1.5 and Mauna Kea ground-based “daytime–nighttime” ClO profiles. SMILES data shown in magenta are those smoothed to the ground-based vertical resolution using the averaging kernel and the a priori profile of the ground-based measurements. Black profile is the original SMILES “daytime–nighttime” ClO profile before smoothing (same as shown in Fig. 13). The green circles are the ground-based measurements with error bars for the $1\text{-}\sigma$ retrieval errors. The lower right panel shows the absolute difference between the smoothed SMILES and the ground-based profiles. Legend on this lower right panel corresponds to the starting day of the observation period.

data showed 0.4 ppbv (30 %) larger VMRs at 50 hPa compared to the JAXA v2.1 product. This issue should be solved in the next version of the NICT level processing, implementing a broader spectral bandwidth in the data analysis.

The comparisons of SMILES NICT v2.1.5 ClO profile with those of Aura MLS (version 3.3) and Odin SMR (Chalmers level-2 version 2.1) were carried out for the low and middle latitude region in order to verify the SMILES data quality at different local times. The SMILES ClO daytime profiles agree well (differences within 0.04 ppbv at the pressure range of 80–2 hPa) with those of MLS after correcting for the known negative bias of MLS. Comparison with the Odin SMR data pointed out that SMR ClO profiles have a negative bias in the mesosphere (0.1 hPa). The difference between SMILES and SMR ClO profiles were fairly consistent with the findings of previous MLS–SMR comparisons. The daytime ClO data from the Envisat MIPAS (version V5R_CIO_220 of the IMK/IAA product) were also used as the comparison data sets. Their differences, -10 to $+60$ pptv, were within the $1\text{-}\sigma$ level of the combined systematic errors. We compared the SMILES ClO profiles inside the polar vortex with those measured by TELIS and MIPAS-B. Despite its degraded sensitivity to the lower stratosphere, the NICT v2.1.5 product of the SMILES ClO profiles detected the ClO enhancement (~ 2.5 ppbv at 25 hPa) to a satisfactory extent. This observed enhancement was slightly larger than those of TELIS and MIPAS-B,

although differences in the observation geometries and horizontal resolutions should be taken into account for further quantitative discussion. In addition, we also found that the “daytime–nighttime” ClO profiles of SMILES have agreement with the “daytime–nighttime” ClO profiles measured by the ground-based instrument at Mauna Kea, which differences are within $1\text{-}\sigma$ of the expected systematic errors for most of the compared profiles.

In conclusion, we found that the NICT-processed SMILES ClO profiles generally agree well with other measurements. No significant bias as a function of local time was detected outside the polar region. This means that the SMILES data set can be scientifically used as a reference for the diurnal variation of ClO. For the lower stratosphere in the nighttime (altitudes below 30 hPa level) and inside the chlorine-activated polar vortex, the current version of the SMILES NICT ClO product shows biases probably due to the configuration in the retrieval analysis. The future versions of the NICT level-2 processing will target this problem. Because of the good agreement between NICT and JAXA products from the middle stratosphere to the mesosphere, we believe that the new version will not significantly improve the results at these altitudes. We conclude that the presented version of SMILES NICT ClO data can be used at pressure $\leq \sim 30$ hPa for scientific analysis.

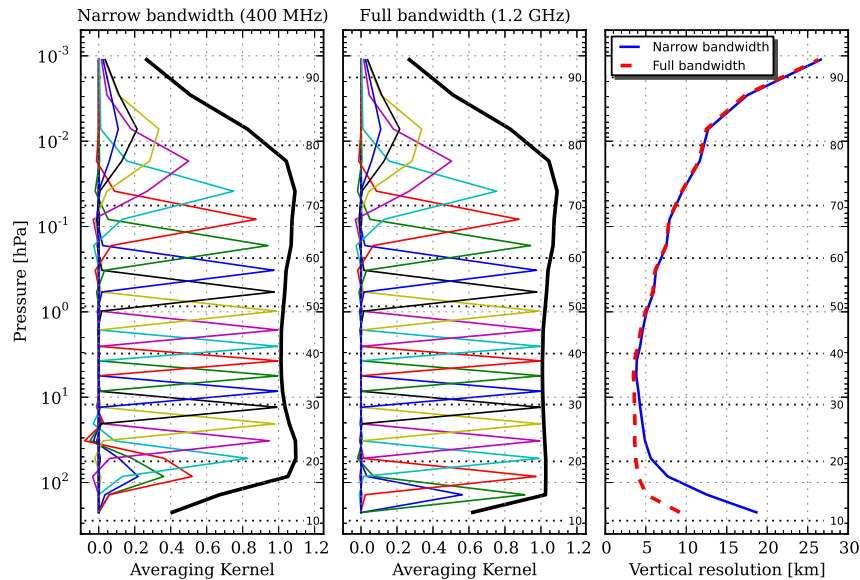


Fig. A1. Theoretical sensitivity of SMILES ClO observation, for a single scan, using different spectral bandwidths in the retrieval analysis. Left panel shows the averaging kernels and the measurement response (bold black) for 400 MHz bandwidth condition which is same with the one used in the NICT v2.1.5 level-2 processing. Middle panel shows the same but for the full bandwidth (1.2 GHz) configuration. Right panel shows the vertical resolutions for the narrow (400 MHz) and full bandwidth simulations.

Appendix A

Impact of the spectral bandwidth on retrieval analysis

The impact of the spectral bandwidth which is used in the SMILES ClO retrieval was investigated by theoretical sensitivity calculations using the averaging kernels. Figure A1 shows the simulated averaging kernels of ClO retrieval when using 400 MHz bandwidth (same condition with the NICT v2.1.5 level-2 processing) and when using 1.2 GHz full width of the Band-C spectrum. The simulation was done with ClO characteristics and measurement noises identical to those used in the NICT v2.1.5 processing, that is, ClO a priori from the daytime mid-latitude condition with a priori uncertainty of $0.5 \times x_a + 2.0 \times 10^{-10}$ (cf. Eq. 16 given by Sato et al., 2012) and the measurement noise of 0.5 K for each frequency channel. For the narrow spectral bandwidth case, the measurement response rapidly decreases at pressure ≥ 50 hPa (altitudes below 20 km). The use of the full 1.2 GHz bandwidth clearly improves the sensitivity at such low altitudes. Limiting the spectral bandwidth makes also the vertical resolution worse in the upper troposphere and lower stratosphere (UT/LS) which explains the actual difference between the NICT and JAXA level-2 ClO products (Fig. 5). Another point to note is that this simulation indicates that there is no significant impact of widening the bandwidth on ClO retrievals at the pressure level $\leq \sim 30$ hPa. In practice, using the narrow bandwidth helps in better-fitting the spectral baseline and reduces the errors from interfering other spectral lines and instrumental ripples (Baron et al., 2011).

Acknowledgements. SMILES is a collaborative project of the National Institute of Information and Communications Technology (NICT) and the Japan Aerospace Exploration Agency (JAXA). The SMILES NICT level-2 data processing was supported by J. Möller (Molflow Co., Ltd.) and by K. Muranaga and T. Haru (SEC Co., Ltd.). The author HS is grateful to C. Mitsuda (Fujitsu F. I. P. Corp.) and the SMILES level-2 team in JAXA for their valuable discussions on the SMILES internal comparison. Work at the Jet Propulsion Laboratory, California Institute of Technology was performed under contract with the National Aeronautics and Space Administration. Odin is a Swedish-led satellite project funded jointly by Sweden (SNSB), Canada (CSA), Finland (TEKES), France (CNES), and the Third Party Mission program of the European Space Agency (ESA). TELIS is a collaboration project of the Deutsche Zentrum für Luft- und Raumfahrt (DLR) in Germany, the Rutherford Appleton Laboratory (RAL) in the UK, and the Netherlands Institute for Space Research (SRON) in the Netherlands. We are grateful to the MIPAS balloon team at Karlsruhe Institute of Technology (KIT), the TELIS balloon team at DLR and SRON, and the Swedish Space Corporation (SSC) Esrange people for excellent balloon operations and data processing. The ground-based data used in this publication were obtained as part of the Network for the Detection of Atmospheric Composition Change (NDACC) and are publicly available (<http://www.ndacc.org>). The author TOS is supported by a Grant in Aid for Research Fellowship for Young Scientists DC1 (no. 23-9766) from the Japan Society for the Promotion of Science.

Edited by: R. Schofield

References

- Baron, P., Ricaud, P., de La Noë, J., Eriksson, J. E. P., Merino, F., Ridal, M., and Murtagh, D. P.: Studies for the Odin sub-millimetre radiometer. II. Retrieval methodology, *Can. J. Phys.*, 80, 341–356, doi:10.1139/p01-150, 2002.
- Baron, P., Urban, J., Sagawa, H., Möller, J., Murtagh, D. P., Mendrok, J., Dupuy, E., Sato, T. O., Ochiai, S., Suzuki, K., Manabe, T., Nishibori, T., Kikuchi, K., Sato, R., Takayanagi, M., Murayama, Y., Shiotani, M., and Kasai, Y.: The Level 2 research product algorithms for the Superconducting Submillimeter-Wave Limb-Emission Sounder (SMILES), *Atmos. Meas. Tech.*, 4, 2105–2124, doi:10.5194/amt-4-2105-2011, 2011.
- Barret, B., Ricaud, P., Santee, M. L., Attié, J.-L., Urban, J., Le Flochmoën, E., Berthet, G., Murtagh, D., Eriksson, P., Jones, A., de La Noë, J., Dupuy, E., Froidevaux, L., Livesey, N. J., Waters, J. W., and Filipiak, M. J.: Intercomparisons of trace gases profiles from the Odin/SMR and Aura/MLS limb sounders, *J. Geophys. Res.*, 111, D21302, doi:10.1029/2006JD007305, 2006.
- Birk, M., Wagner, G., de Lange, G., de Lange, A., Ellison, B. N., Harman, M. R., Murk, A., Oelhaf, H., Maucher, G., and Sartorius, C.: TELIS: TERAhertz and subMMW Limb Sounder – Project Summary After First Successful Flight, in: Twenty-First International Symposium on Space Terahertz Technology, 195–200, 2010.
- Cohen, E. A., Pickett, H. M., and Geller, M.: The submillimeter spectrum of ClO, *J. Mol. Spectrosc.*, 106, 430–435, doi:10.1016/0022-2852(84)90173-5, 1984.
- Connor, B. J., Mooney, T., Barrett, J., Solomon, P., Parrish, A., and Santee, M.: Comparison of ClO measurements from the Aura Microwave Limb Sounder to ground-based microwave measurements at Scott Base, Antarctica, in spring 2005, *J. Geophys. Res.*, 112, D24S42, doi:10.1029/2007JD008792, 2007.
- Connor, B. J., Mooney, T., Nedoluha, G. E., Barrett, J. W., Parrish, A., Koda, J., Santee, M. L., and Gomez, R. M.: Re-analysis of ground-based microwave ClO measurements from Mauna Kea, 1992 to early 2012, *Atmos. Chem. Phys.*, 13, 8643–8650, doi:10.5194/acp-13-8643-2013, 2013.
- de Lange, A., Birk, M., de Lange, G., Friedl-Vallon, F., Kiselev, O., Koshelets, V., Maucher, G., Oelhaf, H., Selig, A., Vogt, P., Wagner, G., and Landgraf, J.: HCl and ClO in activated Arctic air; first retrieved vertical profiles from TELIS submillimetre limb spectra, *Atmos. Meas. Tech.*, 5, 487–500, doi:10.5194/amt-5-487-2012, 2012.
- de Lange, G., Birk, M., Boersma, D., Dercksen, J., Dmitriev, P., Ermakov, A. B., Filippenko, L. V., Golstein, H., Hoogeveen, R. W. M., de Jong, L., Khudchenko, A. V., Kinev, N. V., Kiselev, O. S., van Kuik, B., de Lange, A., van Rantwijk, J., Selig, A. M., Sobolev, A. S., Torgashin, M. Y., de Vries, E., Wagner, G., Yagoubov, P. A., and Koshelets, V. P.: Development and characterization of the superconducting integrated receiver channel of the TELIS atmospheric sounder, *Supercond. Sci. Tech.*, 23, 045016, doi:10.1088/0953-2048/23/4/045016, 2010.
- Dupuy, E., Walker, K. A., Kar, J., Boone, C. D., McElroy, C. T., Bernath, P. F., Drummond, J. R., Skelton, R., McLeod, S. D., Hughes, R. C., Nowlan, C. R., Dufour, D. G., Zou, J., Nichitiu, F., Strong, K., Baron, P., Bevilacqua, R. M., Blumenstock, T., Bodeker, G. E., Borsdorff, T., Bourassa, A. E., Bovensmann, H., Boyd, I. S., Bracher, A., Brogniez, C., Burrows, J. P., Catoire, V., Ceccherini, S., Chabrillat, S., Christensen, T., Coffey, M. T., Cortesi, U., Davies, J., De Clercq, C., Degenstein, D. A., De Mazière, M., Demoulin, P., Dodion, J., Firanski, B., Fischer, H., Forbes, G., Froidevaux, L., Fussen, D., Gerard, P., Godin-Beekmann, S., Goutail, F., Granville, J., Griffith, D., Haley, C. S., Hannigan, J. W., Höpfner, M., Jin, J. J., Jones, A., Jones, N. B., Jucks, K., Kagawa, A., Kasai, Y., Kerzenmacher, T. E., Kleinböhl, A., Klekociuk, A. R., Kramer, I., Küllmann, H., Kuttippurath, J., Kyrölä, E., Lambert, J.-C., Livesey, N. J., Llewellyn, E. J., Lloyd, N. D., Mahieu, E., Manney, G. L., Marshall, B. T., McConnell, J. C., McCormick, M. P., McDermaid, I. S., McHugh, M., McLinden, C. A., Mellqvist, J., Mizutani, K., Murayama, Y., Murtagh, D. P., Oelhaf, H., Parrish, A., Petelina, S. V., Piccolo, C., Pommereau, J.-P., Randall, C. E., Robert, C., Roth, C., Schneider, M., Senten, C., Steck, T., Strandberg, A., Strawbridge, K. B., Sussmann, R., Swart, D. P. J., Tarasick, D. W., Taylor, J. R., Tétard, C., Thomason, L. W., Thompson, A. M., Tully, M. B., Urban, J., Vanhellemont, F., Vigouroux, C., von Clarmann, T., von der Gathen, P., von Savigny, C., Waters, J. W., Witte, J. C., Wolff, M., and Zawodny, J. M.: Validation of ozone measurements from the Atmospheric Chemistry Experiment (ACE), *Atmos. Chem. Phys.*, 9, 287–343, doi:10.5194/acp-9-287-2009, 2009.
- Fischer, H., Birk, M., Blom, C., Carli, B., Carlotti, M., von Clarmann, T., Delbouille, L., Dudhia, A., Ehhalt, D., Endemann, M., Flaud, J. M., Gessner, R., Kleinert, A., Koopman, R., Langen, J., López-Puertas, M., Mosner, P., Nett, H., Oelhaf, H., Perron, G., Remedios, J., Ridolfi, M., Stiller, G., and Zander, R.: MIPAS: an instrument for atmospheric and climate research, *Atmos. Chem. Phys.*, 8, 2151–2188, doi:10.5194/acp-8-2151-2008, 2008.
- Friedl-Vallon, F., Maucher, G., Seefeldner, M., Trieschmann, O., Kleinert, A., Lengel, A., Keim, C., Oelhaf, H., and Fischer, H.: Design and Characterization of the Balloon-Borne Michelson Interferometer for Passive Atmospheric Sounding (MIPAS-B2), *Appl. Optics*, 43, 3335–3355, doi:10.1364/AO.43.003335, 2004.
- Glatthor, N., von Clarmann, T., Fischer, H., Grabowski, U., Höpfner, M., Kellmann, S., Kiefer, M., Linden, A., Milz, M., Steck, T., Stiller, G. P., Mengistu Tsidu, G., Wang, D.-Y., and Funke, B.: Spaceborne ClO observations by the Michelson Interferometer for Passive Atmospheric Sounding (MIPAS) before and during the Antarctic major warming in September/October 2002, *J. Geophys. Res.*, 109, D11307, doi:10.1029/2003JD004440, 2004.
- Hedin, A. E.: Extension of the MSIS thermosphere model into the middle and lower atmosphere, *J. Geophys. Res.*, 96, 1159–1172, doi:10.1029/90JA02125, 1991.
- Khosravi, M., Baron, P., Urban, J., Froidevaux, L., Jonsson, A. I., Kasai, Y., Kuribayashi, K., Mitsuda, C., Murtagh, D. P., Sagawa, H., Santee, M. L., Sato, T. O., Shiotani, M., Suzuki, M., von Clarmann, T., Walker, K. A., and Wang, S.: Diurnal variation of stratospheric and lower mesospheric HOCl, ClO and HO₂ at the equator: comparison of 1-D model calculations with measurements by satellite instruments, *Atmos. Chem. Phys.*, 13, 7587–7606, doi:10.5194/acp-13-7587-2013, 2013.
- Kikuchi, K., Nishibori, T., Ochiai, S., Ozeki, H., Irinajiri, Y., Kasai, Y., Koike, M., Manabe, T., Mizukoshi, K., Murayama, Y., Nagahama, T., Sano, T., Sato, R., Seta, M., Takahashi, C., Takayanagi, M., Masuko, H., Inatani, J., Suzuki, M., and Shiotani, M.: Overview and early results of the Superconducting Submillimeter-Wave Limb-Emission Sounder (SMILES),

- J. Geophys. Res., 115, D23306, doi:10.1029/2010JD014379, 2010.
- Livesey, J. N., Read, W. G., Froidevaux, L., Lambert, A., Manney, G. L., Pumphrey, H. C., Santee, M. L., Schwartz, M. J., Wang, S., Cofield, R. E., Cuddy, D. T., Fuller, R. A., Jarnot, R. F., Jiang, J. H., Knosp, B. W., Stek, P. C., Wagner, P. A., and Wu, D. L.: Version 3.3 Level 2 data quality and description document., Tech. Rep. JPL D-33509, Jet Propulsion Laboratory, available at: <http://mls.jpl.nasa.gov/data/datadocs.php> (last access: 18 October 2013), 2011.
- Livesey, N. J., van Snyder, W., Read, W. G., and Wagner, P. A.: Retrieval Algorithms for the EOS Microwave Limb Sounder (MLS), IEEE T. Geosci. Remote Sens., 44, 1144–1155, doi:10.1109/TGRS.2006.872327, 2006.
- Manney, G. L., Daffer, W. H., Zawodny, J. M., Bernath, P. F., Hopfel, K. W., Walker, K. A., Knosp, B. W., Boone, C., Remsburg, E. E., Santee, M. L., Harvey, V. L., Pawson, S., Jackson, D. R., Deaver, L., McElroy, C. T., McLinden, C. A., Drummond, J. R., Pumphrey, H. C., Lambert, A., Schwartz, M. J., Froidevaux, L., McLeod, S., Takacs, L. L., Suarez, M. J., Trepte, C. R., Cuddy, D. C., Livesey, N. J., Harwood, R. S., and Waters, J. W.: Solar occultation satellite data and derived meteorological products: Sampling issues and comparisons with Aura Microwave Limb Sounder, J. Geophys. Res., 112, D24S50, doi:10.1029/2007JD008709, 2007.
- Merino, F., Murtagh, D. P., Ridal, M., Eriksson, P., Baron, P., Ricaud, P., and de La Noë, J.: Studies for the Odin sub-millimetre radiometer: III. Performance simulations, Can. J. Phys., 80, 357–373, doi:10.1139/p01-154, 2002.
- Mizobuchi, S., Kikuchi, K., Ochiai, S., Nishibori, T., Sano, T., Tamaki, K., and Ozeki, H.: In-orbit measurement of the AOS (Acousto-Optical Spectrometer) response using frequency comb signals, IEEE J. Sel. Topics Appl. Earth Obs. Remote Sens., 5, 977–983, doi:10.1109/JSTARS.2012.2196413, 2012.
- Molina, M. J. and Rowland, F. S.: Stratospheric sink for chlorofluoromethanes: chlorine atom-catalysed destruction of ozone, Nature, 249, 810–812, doi:10.1038/249810a0, 1974.
- Murtagh, D., Frisk, U., Merino, F., Ridal, M., Jonsson, A., Stegman, J., Witt, G., Eriksson, P., Jiménez, C., Megie, G., de La Noë, J., Ricaud, P., Baron, P., Pardo, J. R., Hauchorne, A., Llewellyn, E. J., Degenstein, D. A., Gattinger, R. L., Lloyd, N. D., Evans, W. F. J., McDade, I. C., Haley, C. S., Sioris, C., von Savigny, C., Solheim, B. H., McConnell, J. C., Strong, K., Richardson, E. H., Leppelmeier, G. W., Kyrölä, E., Auvinen, H., and Oikarinen, L.: An overview of the Odin atmospheric mission, Can. J. Phys., 80, 309–318, doi:10.1139/p01-157, 2002.
- Nedoluha, G. E., Connor, B. J., Barrett, J., Mooney, T., Parrish, A., Boyd, I., Wrotny, J. E., Gomez, R. M., Koda, J., Santee, M. L., and Froidevaux, L.: Ground-based measurements of ClO from Mauna Kea and intercomparisons with Aura and UARS MLS, J. Geophys. Res., 116, D02307, doi:10.1029/2010JD014732, 2011.
- Ochiai, S., Kikuchi, K., Nishibori, T., Manabe, T., Ozeki, H., Mizukoshi, K., Ohtsubo, F., Tsubosaka, K., Irimajiri, Y., Sato, R., and Shiotani, M.: Performance of JEM/SMILES in Orbit, in: Twenty-First International Symposium on Space Terahertz Technology, 179–184, 2010.
- Oh, J. and Cohen, E. A.: Pressure broadening of ClO by N₂ and O₂ near 204 and 649 GHz and new frequency measurements between 632 and 725 GHz, J. Quant. Spectrosc. Ra., 52, 151–156, doi:10.1016/0022-4073(94)90004-3, 1994.
- Pardo, J. R., Serabyn, E., and Cernicharo, J.: Submillimeter atmospheric transmission measurements on Mauna Kea during extremely dry El Niño conditions: implications for broadband opacity contributions, J. Quant. Spectrosc. Ra., 68, 419–433, 2001.
- Pickett, H. M., Poynter, R. L., Cohen, E. A., Delitsky, M. L., Pearson, J. C., and Müller, H. S. P.: Submillimeter, millimeter and microwave spectral line catalog., J. Quant. Spectrosc. Ra., 60, 883–890, doi:10.1016/S0022-4073(98)00091-0, 1998.
- Reber, C. A., Trevathan, C. E., McNeal, R. J., and Luther, M. R.: The Upper Atmosphere Research Satellite (UARS) mission, J. Geophys. Res., 98, 10643, doi:10.1029/92JD02828, 1993.
- Rienecker, M. M., Suarez, M. J., Todling, R., Bacmeister, J., Takacs, L., Liu, H.-C., Gu, W., Sienkiewicz, M., Koster, R. D., Gelaro, R., Stajner, I., and Nielsen, J. E.: The GEOS-5 Data Assimilation System—Documentation of Versions 5.0.1, 5.1.0, and 5.2.0., Tech. Rep. NASA/TM-2008-104606, Vol. 27, National Aeronautics and Space Administration, available at: <http://mls.jpl.nasa.gov/data/datadocs.php> (last access: 18 October 2013), 2008.
- Rodgers, C. D.: Retrieval of Atmospheric Temperature and Composition From Remote Measurements of Thermal Radiation, Rev. Geophys. Space Phys., 14, 609–624, 1976.
- Rodgers, C. D.: Characterization and error analysis of profiles retrieved from remote sounding measurements, J. Geophys. Res., 95, 5587–5595, doi:10.1029/JD095iD05p05587, 1990.
- Rodgers, C. D.: Inverse methods for atmospheric sounding: Theory and Practice, Series on atmospheric, oceanic and planetary physics, World Scientific, 2, 3605–3609, 2000.
- Rodgers, C. D. and Connor, B. J.: Intercomparison of remote sounding instruments, J. Geophys. Res., 108, 4116, doi:10.1029/2002JD002299, 2003.
- Santee, M. L., Lambert, A., Read, W. G., Livesey, N. J., Manney, G. L., Cofield, R. E., Cuddy, D. T., Daffer, W. H., Drouin, B. J., Froidevaux, L., Fuller, R. A., Jarnot, R. F., Knosp, B. W., Perun, V. S., Snyder, W. V., Stek, P. C., Thurstans, R. P., Wagner, P. A., Waters, J. W., Connor, B., Urban, J., Murtagh, D., Ricaud, P., Barret, B., Kleinböhl, A., Kuttippurath, J., Küllmann, H., von Hobe, M., Toon, G. C., and Stachnik, R. A.: Validation of the Aura Microwave Limb Sounder ClO measurements, J. Geophys. Res., 113, D15S22, doi:10.1029/2007JD008762, 2008.
- Sato, T. O., Sagawa, H., Kreyling, D., Manabe, T., Ochiai, S., Kikuchi, K., Baron, P., Mendrok, J., Urban, J., Murtagh, D., Yasui, M., and Kasai, Y.: Strato-mesospheric ClO observations by SMILES: error analysis and diurnal variation, Atmos. Meas. Tech., 5, 2809–2825, doi:10.5194/amt-5-2809-2012, 2012.
- Solomon, P., Barrett, J., Mooney, T., Connor, B., Parrish, A., and Siskind, D. E.: Rise and decline of active chlorine in the stratosphere, Geophys. Res. Lett., 33, L18807, doi:10.1029/2006GL027029, 2006.
- Solomon, P. M., de Zafra, R., Parrish, A., and Barrett, J. W.: Diurnal Variation of Stratospheric Chlorine Monoxide: A Critical Test of Chlorine Chemistry in the Ozone Layer, Science, 224, 1210–1214, doi:10.1126/science.224.4654.1210, 1984.
- Suzuki, M., Mitsuda, C., Kikuchi, K., Nishibori, T., Ochiai, S., Ozeki, H., Sano, T., Mizobuchi, S., Takahashi, C., Manago, N., Imai, K., Naito, Y., Hayashi, H., Nishimoto, E., and Shiotani, M.: Overview of the Superconducting Submillimeter-Wave Limb-Emission Sounder (SMILES) and Sensitivity to

- Chlorine Monoxide, ClO, *IEEJ Transactions on Fundamentals and Materials*, 132, 609–615, doi:10.1541/ieejfms.132.609, 2012.
- Tikhonov, A.: On the solution of incorrectly stated problems and a method of regularization, *Dokl. Akad. Nauk SSSR*, 151, 501–504, 1963.
- Urban, J., Lantié, N., Le Flochmoën, E., Jiménez, C., Eriksson, P., de La Noë, J., Dupuy, E., Ekström, M., El Amraoui, L., Frisk, U., Murtagh, D., Olberg, M., and Ricaud, P.: Odin/SMR limb observations of stratospheric trace gases: Level 2 processing of ClO, N₂O, HNO₃, and O₃, *J. Geophys. Res.*, 110, D14307, doi:10.1029/2004JD005741, 2005.
- Urban, J., Murtagh, D., Lantié, N., Barret, B., Dupuy, E., de LaNoë, J., Eriksson, P., Frisk, U., Jones, A., Le Flochmoën, E., Olberg, M., Piccolo, C., Ricaud, P., and Rösevall, J.: Odin/SMR Limb Observations of Trace Gases in the Polar Lower Stratosphere during 2004–2005, in: *Atmospheric Science Conference*, Vol. 628 of ESA Special Publication, 2006.
- von Clarmann, T., Glatthor, N., Höpfner, M., Kellmann, S., Ruhnke, R., Stiller, G. P., Fischer, H., Funke, B., Gil-López, S., and López-Puertas, M.: Experimental evidence of perturbed odd hydrogen and chlorine chemistry after the October 2003 solar proton events, *J. Geophys. Res.*, 110, A09S45, doi:10.1029/2005JA011053, 2005.
- von Clarmann, T., Höpfner, M., Kellmann, S., Linden, A., Chauhan, S., Funke, B., Grabowski, U., Glatthor, N., Kiefer, M., Schieferdecker, T., Stiller, G. P., and Versick, S.: Retrieval of temperature, H₂O, O₃, HNO₃, CH₄, N₂O, ClONO₂ and ClO from MIPAS reduced resolution nominal mode limb emission measurements, *Atmos. Meas. Tech.*, 2, 159–175, doi:10.5194/amt-2-159-2009, 2009.
- Waters, J. W., Froidevaux, L., Read, W. G., Manney, G. L., Elson, L. S., Flower, D. A., Jarnot, R. F., and Harwood, R. S.: Stratospheric ClO and ozone from the Microwave Limb Sounder on the Upper Atmosphere Research Satellite, *Nature*, 362, 597–602, doi:10.1038/362597a0, 1993.
- Waters, J. W., Froidevaux, L., Harwood, R. S., Jarnot, R. F., Pickett, H. M., Read, W. G., Siegel, P. H., Cofield, R. E., Filipiak, M. J., Flower, D. A., Holden, J. R., Lau, G. K., Livesey, N. J., Manney, G. L., Pumphrey, H. C., Santee, M. L., Wu, D. L., Cuddy, D. T., Lay, R. R., Loo, M. S., Perun, V. S., Schwartz, M. J., Stek, P. C., Thurstans, R. P., Boyles, M. A., Chandra, K. M., Chavez, M. C., Chen, G.-S., Chudasama, B. V., Dodge, R., Fuller, R. A., Girard, M. A., Jiang, J. H., Jiang, Y., Knosp, B. W., Labelle, R. C., Lam, J. C., Lee, A. K., Miller, D., Oswald, J. E., Patel, N. C., Pukala, D. M., Quintero, O., Scaff, D. M., Vansnyder, W., Tope, M. C., Wagner, P. A., and Walch, M. J.: The Earth Observing System Microwave Limb Sounder (EOS MLS) on the Aura Satellite, *IEEE T. Geosci. Remote*, 44, 1075–1092, doi:10.1109/TGRS.2006.873771, 2006.
- Wetzel, G., Oelhaf, H., Kirner, O., Friedl-Vallon, F., Ruhnke, R., Ebersoldt, A., Kleinert, A., Maucher, G., Nordmeyer, H., and Orphal, J.: Diurnal variations of reactive chlorine and nitrogen oxides observed by MIPAS-B inside the January 2010 Arctic vortex, *Atmos. Chem. Phys.*, 12, 6581–6592, doi:10.5194/acp-12-6581-2012, 2012.